

# Flow of a visco-plastic fluid in a channel of slowly varying width

I.A. Frigaard

*Department of Mathematics and Department of Mechanical Engineering,  
University of British Columbia, 2324 Main Mall, Vancouver, BC, Canada, V6T  
1Z4.*

D.P. Ryan

*Department of Mathematics, University of British Columbia, 1984 Mathematics  
Road, Vancouver, BC, Canada, V6T 1Z2.*

---

## Abstract

We develop an asymptotic solution for the Poiseuille flow of a Bingham fluid down a channel of slowly varying width, for the case of small amplitude width variation,  $h$ . We show that an asymptotic solution with an intact unyielded plug region can be found for  $h$  less than a critical value  $h_c \sim O(\delta)$ , where  $\delta$  is the aspect ratio, (channel half-width to wavelength of the variation). Our method involves no form of relaxation of the exact Bingham model.

We provide upper and lower estimates for  $h_c$ . The function  $h_c/\delta$  shows little variation with  $\delta \ll 1$ , and exhibits a maximum in Bingham number,  $B$ , at around  $B \approx 5$ . There is a small variation in the true plug speed from that of the uniform channel flow. At small  $B$  the perturbed plug moves slightly slower than that in the uniform channel, whereas at large  $B$  the true plug moves faster than the uniform channel flow. Finally, we consider the structure of the flow for  $h \sim O(1)$ , for which the plug has broken.

*Key words:* Lubrication theory, visco-plastic fluids, extensional flows, pseudo-yield surfaces, pseudo-plugs

---

## 1 Introduction

In this paper we develop an asymptotic solution for the Poiseuille flow of a Bingham fluid down a channel of slowly varying width, for the case of small amplitude width variation,  $h$ , see Fig. 1. The flow of a Newtonian fluid along

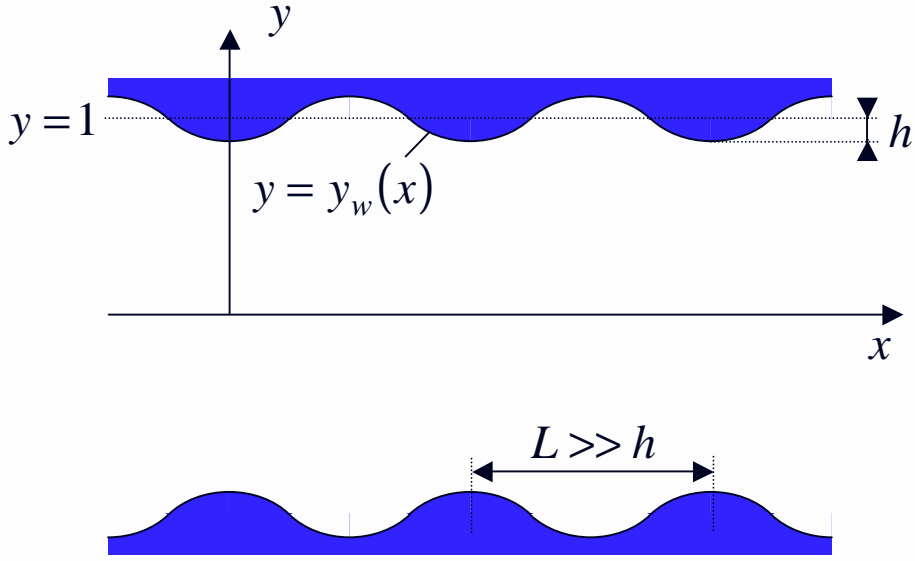


Fig. 1. Slowly varying channel geometry.

a wavy-walled rigid channel, in its various limits, has been studied by many authors, and has effectively become a textbook problem. For a Bingham fluid these same problems can of course be attempted, but here we have a specific objective in mind: namely, to understand what happens to the unyielded plug region under a small perturbation of the channel width.

Analyses of visco-plastic fluid flows in geometries of small aspect ratio have a relatively long history. Part of the interest is in what has become known as the *lubrication paradox* for yield stress fluids, which refers to the existence or non-existence of a true unyielded plug region. It was perhaps Lipscomb & Denn, [1], who first aroused interest in this question by arguing that true rigid plug regions should not exist in complex geometries, with reference to a squeeze flow. The argument is that adoption of classical lubrication, (or thin-film), scaling techniques leads to prediction of a *plug-speed* which varies slowly in the principal flow direction. This variation implies that the plug region cannot be truly unyielded. Such regions have been termed *pseudo-plug* regions and the boundaries either *pseudo-yield* surfaces or *fake yield* surfaces.

There have been a number of attempts to resolve the paradox. Certainly, both analytical and computational methods have shown that true unyielded plugs can exist in complex geometries. The chief value of [1] was however to draw attention to the potential difficulties of these flows, rather than offering a resolution. Probably the earliest demonstration of a true unyielded plug in a slowly varying complex geometry was by Walton & Bittleston, [2], who studied the axial flow of a Bingham fluid along an eccentric annular duct. It was shown analytically, [2], (and later confirmed computationally, [3]), that a true plug can persist in the middle of the channel, on both the wide and narrow side of the eccentric annulus. Between the two rigid plug zones there exists a pseudo-plug region, where the scaled velocity gradient is asymptotically small in the shear direction, (across the annulus), but exhibits an order unity variation in the extensional direction, (the azimuthal direction). What is noteworthy

about these two papers is that both the analytical method and the numerical method, (in [3], but not that in [2]), do not rely on any form of regularisation (or smoothing) of the effective viscosity of the exact Bingham model.

In the context of the lubrication paradox, squeeze flow problems have attracted considerable attention over the years, e.g. [1,4–10]. In an axisymmetric geometry, it may be shown by symmetry arguments that true plug regions exist in an  $O(1)$  region close to the axis of symmetry, at the stagnation points, see [10]. True plugs do not however exist in the radially developing shear flow. In the shear flow region, the mean velocity decreases slowly with radial distance. Thus, there is an imposed extensional strain and this prevents formation of a true plug.

A similar situation is found in thin film flows of visco-plastic fluids down inclined planes, of which there are many practical examples, e.g. [11–26], stemming from both geophysical and industrial scenarios. In these flows there is generally a slow variation in film thickness in the direction of flow. Since the film height determines the leading order velocity solution, there is again a slow extensional stretching of the (pseudo-)plug velocity in the flow direction and no true plug. An exception to this is when the layers become so thin that they do not move. In this situation, the pseudo-plug velocity is zero everywhere and hence the troublesome extensional gradient is removed.

There have been two attempts at an asymptotic analysis of these flows, to resolve the lubrication paradox: by S.D.R. Wilson, [20], and by Balmforth & Craster, [19]. The former method relies on relaxation of the exact Bingham model to a bi-viscosity model, followed by consideration of a distinguished limit of the bi-viscous model. We review Wilson’s method later in the context of our results, in §5. The latter method, [19], is more in the spirit of our analysis, and the earlier analysis in [2]. No relaxation/regularisation is used, (or needed). The results are thus fully consistent with the exact Bingham model.

We consider perturbation of a plane channel Poiseuille flow of a Bingham fluid, via slow length-wise variation of the channel width. In a uniform channel, the Poiseuille flow has a finite width unyielded plug region. For an infinitesimal perturbation of the channel width, (i.e. about the uniform width), one would expect that the unyielded plug will remain. This might appear to be in contradiction to the above analyses of slowly varying shear flows, both in squeeze films and in thin film flows down an incline. However as we have explained, in the above two cases there is a persistent variation of the velocity in the flow direction, i.e. an extensional rate of strain, that does not change sign along in the flow direction. For a channel flow, with periodic variation of the channel width, the extensional strain rate should change sign along the channel. This allows the plug to persist for small amplitude wall variations, as we shall

demonstrate.

An outline of the paper is as follows. A brief introduction to the lubrication model is given below in §2. Section 3 is the main section of the paper and develops the asymptotic approximation for small amplitude width variations. Eventual breaking of the plug and prediction of the critical amplitude is in §4, and we also discuss the flow structure after the plug has broken. In §5 we review the method of distinguished limits for the bi-viscous model, as applied to our situation. The paper concludes with a brief discussion.

## 2 Flow of a visco-plastic fluid in a channel of slowly varying width

The two-dimensional flow of an incompressible Bingham fluid down a channel of slowly varying width is governed by the following dimensionless equations:

$$Re\left(\frac{\partial u^*}{\partial t^*} + u^* \frac{\partial u^*}{\partial x^*} + v^* \frac{\partial u^*}{\partial y^*}\right) = -\frac{\partial p^*}{\partial x^*} + \frac{\partial}{\partial x^*} \tau_{xx}^* + \frac{\partial}{\partial y^*} \tau_{xy}^* \quad (1)$$

$$Re\left(\frac{\partial v^*}{\partial t^*} + u^* \frac{\partial v^*}{\partial x^*} + v^* \frac{\partial v^*}{\partial y^*}\right) = -\frac{\partial p^*}{\partial y^*} + \frac{\partial}{\partial x^*} \tau_{xy}^* + \frac{\partial}{\partial y^*} \tau_{yy}^* \quad (2)$$

$$\frac{\partial u^*}{\partial x^*} + \frac{\partial v^*}{\partial y^*} = 0. \quad (3)$$

Here the  $x^*$ -coordinate is aligned with the channel axis,  $\mathbf{u}^* = (u^*, v^*)$  is the velocity,  $p^*$  is the pressure and  $\tau_{ij}^*$  is the deviatoric stress tensor. The dimensionless parameter  $Re$  is the Reynolds number and a further dimensionless parameter  $B$ , the Bingham number, appears in the constitutive laws:

$$\tau_{ij}^* = \left(1 + \frac{B}{\dot{\gamma}^*}\right) \dot{\gamma}_{ij}^* \iff \tau^* > B \quad (4)$$

$$\dot{\gamma}^* = 0 \iff \tau^* \leq B, \quad (5)$$

where

$$\dot{\gamma}_{xy}^* = \frac{\partial u^*}{\partial y^*} + \frac{\partial v^*}{\partial x^*} = \dot{\gamma}_{yx}^*, \quad \dot{\gamma}_{xx}^* = 2 \frac{\partial u^*}{\partial x^*}, \quad \dot{\gamma}_{yy}^* = 2 \frac{\partial v^*}{\partial y^*}.$$

and (due to symmetry, incompressibility and the fact that  $\tau_{ij}^*$  is deviatoric), we may write

$$\dot{\gamma}^* \equiv \left[\frac{1}{2}(\dot{\gamma}_{ij}^*)^2\right]^{1/2} = [(\dot{\gamma}_{xy}^*)^2 + (\dot{\gamma}_{xx}^*)^2]^{1/2},$$

$$\tau^* \equiv \left[ \frac{1}{2} (\tau_{ij}^*)^2 \right]^{1/2} = [(\tau_{xy}^*)^2 + (\tau_{xx}^*)^2]^{1/2},$$

which leads to some algebraic convenience later. We have chosen the Bingham fluid as the simplest of a class of inelastic visco-plastic fluids, but our analysis below readily extends to other visco-plastic fluid models.

The dimensionless parameters are defined by

$$Re \equiv \frac{\hat{\rho} \hat{U}_0 \hat{D}}{\hat{\mu}}, \quad B \equiv \frac{\hat{\tau}_y \hat{D}}{\hat{\mu} \hat{U}_0}. \quad (6)$$

where  $\hat{\rho}$ ,  $\hat{U}_0$ ,  $\hat{D}$ ,  $\hat{\mu}$  &  $\hat{\tau}_Y$  are respectively the density, mean flow velocity, channel half-width, plastic viscosity and yield stress, (all dimensional). To derive the non-dimensional field equations above, we have scaled length with  $\hat{D}$ , velocity with  $\hat{U}_0$ , pressure and deviatoric stress with  $\hat{\mu} \hat{U}_0 / \hat{D}$ .

The focus of our paper is on the effects of a slowly varying channel width on the basic Poiseuille flow. To simplify matters, we will consider the channel to be symmetric about  $y^* = 0$ , and the channel wall to be sinusoidally perturbed, i.e. the upper wall is at:

$$y^* = y_w^* = 1 - h \cos \frac{2\pi x^*}{L}, \quad L \gg 1. \quad (7)$$

Thus,  $L$  denotes the period of the channel width variation and  $h$  the amplitude. The channel is assumed to extend to  $x^* = \pm\infty$ , although we shall only consider one period of the wall variation. Boundary conditions of no slip are imposed at the wall, and symmetry conditions at the channel centre.

### 2.1 Lubrication approximation

As suggested by the slow channel width variation, we seek a lubrication approximation to full problem. We do this by re-scaling the variables as follows:

$$\begin{array}{lllll} t = t^* & x = \delta x^* & y = y^* & \dot{\gamma}_{xy} = \dot{\gamma}_{xy}^* & \dot{\gamma}_{xx} = \dot{\gamma}_{xx}^* / \delta \\ u = u^* & v = v^* / \delta & p = p^* & \tau_{xy} = \tau_{xy}^* & \tau_{xx} = \tau_{xx}^* / \delta, \end{array}$$

where  $\delta = 1/L \ll 1$ . The approach is standard and yields the following set of equations, which we will study in the remainder of the paper.

$$\delta Re \left( \frac{\partial u}{\partial t} + u \frac{\partial u}{\partial x} + v \frac{\partial u}{\partial y} \right) = -\frac{\partial p}{\partial x} + \delta^2 \frac{\partial}{\partial x} \tau_{xx} + \frac{\partial}{\partial y} \tau_{xy}, \quad (8)$$

$$\delta^3 Re \left( \frac{\partial v}{\partial t} + u \frac{\partial v}{\partial x} + v \frac{\partial v}{\partial y} \right) = -\frac{\partial p}{\partial y} + \delta^2 \frac{\partial}{\partial x} \tau_{xy} + \delta^2 \frac{\partial}{\partial y} \tau_{yy}, \quad (9)$$

$$\frac{\partial u}{\partial x} + \frac{\partial v}{\partial y} = 0. \quad (10)$$

The constitutive laws are still:

$$\tau_{ij} = \left(1 + \frac{B}{\dot{\gamma}}\right) \dot{\gamma}_{ij} \iff \tau > B \quad (11)$$

$$\dot{\gamma} = 0 \iff \tau \leq B, \quad (12)$$

but now

$$\dot{\gamma}_{xy} = \dot{\gamma}_{yx} = \frac{\partial u}{\partial y} + \delta^2 \frac{\partial v}{\partial x}, \quad \dot{\gamma}_{xx} = 2 \frac{\partial u}{\partial x} = -2 \frac{\partial v}{\partial y} = -\dot{\gamma}_{yy}.$$

and

$$\dot{\gamma} = [\dot{\gamma}_{xy}^2 + \delta^2 \dot{\gamma}_{xx}^2]^{\frac{1}{2}}, \quad \tau = [\tau_{xy}^2 + \delta^2 \tau_{xx}^2]^{\frac{1}{2}}. \quad (13)$$

Until now we have made no approximation. In what follows, we shall mostly assume that  $Re \ll 1$ , formally  $Re = O(\delta)$ , in which case inertial effects are negligible. Having developed our analysis, we later consider how it is modified by having  $Re \sim O(1)$ , (see §3.6). For either case, it is evident that a naive first approximation to the flow is that of a symmetric shear flow in a channel with half-width:  $y_w = 1 - h \cos 2\pi x$ . We shall construct our asymptotic solutions about this approximation.

In the case that  $h = 0$ , we have a Poiseuille flow with an unyielded plug in the centre of the channel, but for  $h > 0$  it is unclear what happens to the plug. We have three objectives. First, to show that it is possible, using consistent asymptotic approximations to the Bingham fluid model, to derive an asymptotic approximation to the solution for the case where  $h \sim O(\delta)$ . For sufficiently small  $h/\delta$ , these solutions exhibit an unyielded central plug along the entire length of the channel. Secondly, we show that at some larger  $h/\delta$ , the central plug will break. We provide a prediction of the breaking amplitude and discuss the structure of the flow after the plug has broken, when  $h = O(1)$ . Lastly, we show that the true yield surfaces predicted in our analysis are not compatible with those predicted using Wilson's method of distinguished limits, [20], neither quantitatively nor qualitatively.

### 3 Small amplitude wall variation: $h = O(\delta)$

It is physically intuitive that, as  $h \rightarrow 0$ , the unyielded plug of the underlying basic Poiseuille flow should be recovered in any analysis. Further, since a plug region of finite width in the basic flow is indicative of a finite yield stress, we would expect that for a sufficiently small amplitude channel width perturbation, the plug remains intact along the entire length of the channel, i.e. it is physically unreasonable that an infinitesimal perturbation of the channel wall creates the finite stress required to break the plug at every point. Accordingly, we consider here the case that  $h \ll 1$ , and specifically  $h = O(\delta)$ .

For definiteness, we consider  $x \in [-1/2, 1/2]$ , and assume periodicity in  $x$ . Boundary conditions at the centreline and wall are:

$$\tau_{xy} = 0, \quad v = 0, \quad \text{at } y = 0, \quad (14)$$

$$u = 0, \quad v = 0, \quad \text{at } y = y_w(x) = 1 - h \cos 2\pi x, \quad h = O(\delta). \quad (15)$$

We seek an asymptotic solution with the following structure. First, close to the wall there will exist a yielded region, which to first approximation is a shear flow, (outer solution). Second, in the channel centre there will be a rigid plug, (also an outer solution), moving at speed  $u_p$ , which will be determined. The two outer solutions will be joined at the approximate position of the (naively) perturbed yield surface by an inner solution and matching conditions. We commence with the yielded outer solution.

#### 3.1 Yielded outer solution

We consider regular expansions in  $\delta$  of form:

$$\begin{aligned} p &= p_0 + \delta p_1 + \delta^2 p_2 + \dots, \\ u &= u_0 + \delta u_1 + \delta^2 u_2 + \dots, \\ v &= v_0 + \delta v_1 + \delta^2 v_2 + \dots, \end{aligned}$$

and after a little algebra find the following sequence of problems:

$$O(1) : 0 = -p_{0,x} + \frac{\partial}{\partial y} \tau_{xy,0}, \quad (16)$$

$$0 = p_{0,y}, \quad (17)$$

$$0 = u_{0,x} + v_{0,y}, \quad (18)$$

$$O(\delta) : 0 = -Re[u_0 u_{0,x} + v_0 u_{0,y}] - p_{1,x} + \frac{\partial}{\partial y} \tau_{xy,1}, \quad (19)$$

$$0 = p_{1,y}, \quad (20)$$

$$0 = u_{1,x} + v_{1,y}, \quad (21)$$

$$O(\delta^2) : 0 = -p_{2,x} + \frac{\partial}{\partial y} \tau_{xy,2} + \frac{\partial}{\partial x} \tau_{xx,0}, \quad (22)$$

$$0 = -p_{2,y} + \frac{\partial}{\partial x} \tau_{xy,0} + \frac{\partial}{\partial y} \tau_{yy,0}. \quad (23)$$

$$0 = u_{2,x} + v_{2,y}, \quad (24)$$

The leading order shear stress is given by  $\tau_0 = |\tau_{xy,0}|$  and, provided that  $|\tau_{xy,0}| > B$ , the shear stress components are given by:

$$\begin{aligned} \tau_{xy,0} &= u_{0,y} + B \operatorname{sgn}(u_{0,y}), & \tau_{xy,1} &= u_{1,y}, \\ \tau_{xx,0} &= 2 \left( 1 + \frac{B}{|u_{0,y}|} \right) u_{0,x}, & \tau_{xy,2} &= \left[ u_{2,y} + v_{0,x} - B \operatorname{sgn}(u_{0,y}) \frac{2u_{0,x}^2}{u_{0,y}^2} \right]. \end{aligned}$$

We note that the  $x$ -dependency in (16) enters only through the channel width,  $y_w(x)$ , and thus we can expect that the leading order solution  $(u_0, v_0)$  depends on  $x$  only through  $y_w$ . It follows that

$$u_{0,x} = \frac{\partial u_0}{\partial y_w} y_{w,x} = O(\delta), \quad v_0 = \int_1^y v_{0,y} dy = - \int_1^y u_{0,x} dy = O(\delta).$$

Thus, we note that many of the terms in the leading order deviatoric stresses drop one order, i.e.  $\tau_{xx,0} \sim O(\delta)$  and many terms drop out of  $\tau_{xy,2}$ . We also see that the inertial terms in (19) are in fact  $O(\delta)$ , and belong in the second order equation. Further, we will now assume that  $Re \sim O(\delta)$ , so that the inertial terms in fact appear only at  $O(\delta^3)$ . We consider how inertia modifies our solutions, when  $Re = O(1)$ , later in §3.6.

Substituting for the stress components above, and with our assumptions regarding  $Re$ , we see that  $p = p(x)$ , to second order, and that the  $x$ -momentum equations are replaced by:

$$0 = -p_{0,x} + u_{0,yy}, \quad (25)$$

$$0 = -p_{1,x} + u_{1,yy}, \quad (26)$$

$$0 = -p_{2,x} + u_{2,yy}, \quad (27)$$

These equations are valid where  $|\tau_{xy,0}| > B$ , and where  $|\tau_{xy,0}| \leq B$ , we have simply that  $u_{k,y} = 0$ ,  $k = 0, 1, 2$ .

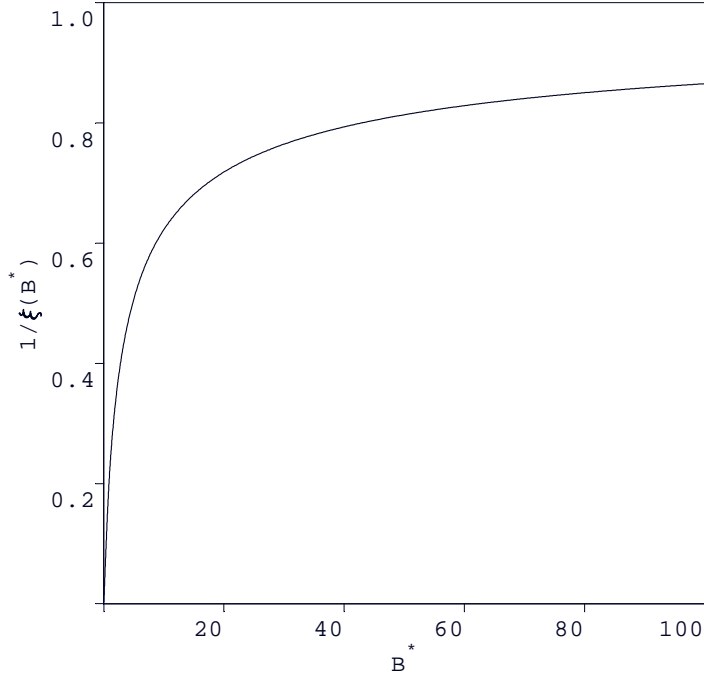


Fig. 2. The function  $\xi(B^*)$  that defines  $y_y(x)$ .

The outer solution is solved straightforwardly, using the boundary conditions  $u_k(x, y_w) = 0$ ,  $k = 0, 1, 2$ , and symmetry at  $y = 0$ . The pressure gradient is determined from the constraint of a unit areal flux in the  $x$ -direction at leading order, (due to scaling with the mean velocity), i.e.

$$\int_0^{y_w} u_0(x, y) dy = 1. \quad (28)$$

At leading order, we have  $\tau_{xy,0} = p_{0,x}y$ , and:

$$u_0(x, y) = \begin{cases} \frac{B}{2y_y}(y_w - y_y)^2 & y \in [0, y_y], \\ \frac{B}{2y_y}(y_w - y_y)^2 \left[ 1 - \frac{(y - y_y)^2}{(y_w - y_y)^2} \right] & y \in (y_y, y_w]. \end{cases} \quad (29)$$

Here

$$y_y = \frac{B}{|p_{0,x}|}, \quad (30)$$

is the position of the pseudo-yield surface, where  $|\tau_{xy,0}| = B$ . However,  $|p_{0,x}|$  is as yet unknown. This is found by integrating (29) across the channel,  $y \in [0, y_w]$ , and using (28). After minor manipulations, we find that

$$y_y = \frac{y_w}{\xi}, \quad (31)$$

where  $\xi = \xi(B^*)$ , is the single root of the Buckingham equation:

$$2\xi^3 - \left(3 + \frac{6}{B^*}\right)\xi^2 + 1 = 0, \quad (32)$$

for which  $\xi > 1$ , and  $B^* = By_w^2$ . On finding the root, (e.g. numerically, see Fig. 2), we can determine  $y_y$ . The pressure gradient is defined by (30), and finally the solution from (29). Thus, the entire leading order solution depends only on  $B$  and on  $y_w(x)$ , as previously stated.

### 3.2 The lubrication paradox illustrated

The zero-th order solution (29), has the characteristic Bingham-Poiseuille velocity profile of a sheared layer with a parabolic variation coupled to a plug region. However, it is evident that the plug region,  $y \in [0, y_y]$ , is not a true plug region, since the leading order velocity varies in the  $x$ -direction. This is the essence of the *lubrication paradox* for yield stress fluids. The explanation of why this happens is straightforward. The axial variation in velocity is characterised by that in the channel centre. We denote the pseudo-plug velocity by  $u_{pp}(x)$ :

$$u_{pp}(x) \equiv u_0(y_y(x)) = \frac{B}{2y_y}(y_w - y_y)^2.$$

Since  $y_w = 1 + O(\delta)$ , we have that  $B^* = B + O(\delta)$ . The root of (32) varies continuously with  $B$ , and therefore  $\xi(B^*) = 1/y_{y,0} + O(\delta)$ , where  $y_{y,0}$  is the yield surface of the uniform Poiseuille flow in a plane channel of half-width 1. It follows that both pseudo-yield surface position,  $y_y(x)$ , and pseudo-plug velocity,  $u_{pp}(x)$ , are  $O(\delta)$  perturbations from the uniform Poiseuille flow values.

The lubrication equations were derived under the assumption that the axial velocity is an order of magnitude larger than that across the channel **and** that all variations in the axial direction are slow in comparison with those across the channel. It is clear that the latter assumption breaks down, but not the former. In our leading order solution we have velocity gradients in  $x$ , of  $O(\delta)$ . These balance with the velocity gradients in  $y$ , at a distance of  $O(\delta)$  from the pseudo-yield surface,  $y_y(x)$ . This is approximately where the outer expansion breaks down.

To illustrate the leading order solution we plot a series of velocity profiles, (Fig. 3a & c), and examine the variation in pseudo-plug velocity along the channel, (Fig. 3b & d). In Fig. 4 we plot the pseudo-yield surface position,  $y_y(x)$ , and the leading order pressure gradient  $p_{0,x}$ , along the channel, for the

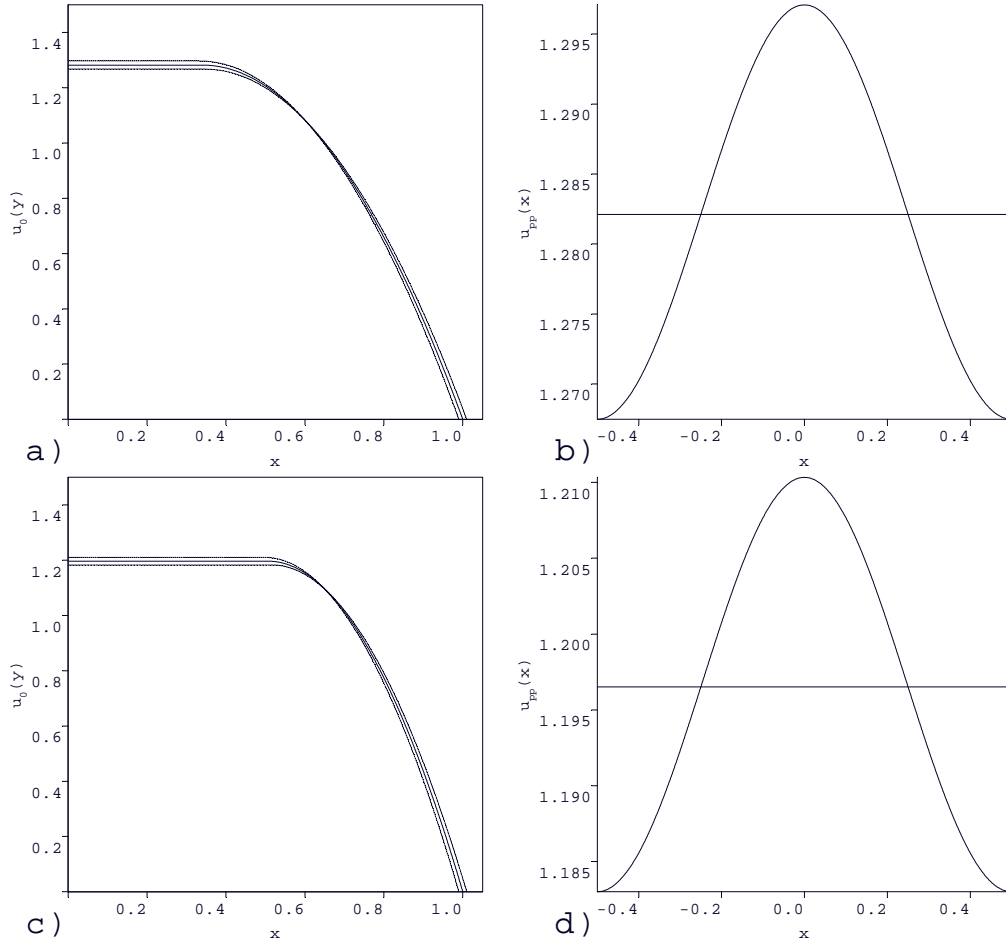


Fig. 3. Leading order outer velocity solution. a) velocity profile at  $x = 0.25$ , and at the maximal and minimal channel widths,  $x = 0$  &  $x = 0.5$ , thick line indicates the uniform Poiseuille flow in the unperturbed channel; b) pseudo-plug velocity  $u_{pp}(x)$ , thick horizontal line indicates the plug velocity in the unperturbed channel; (Parameters for a) & b):  $B = 2$ ,  $\delta = 0.05$ ,  $h = 0.01$ ); c) velocity profile at  $x = 0.25$ , and at the maximal and minimal channel widths,  $x = 0$  &  $x = 0.5$ , thick line indicates the uniform Poiseuille flow in the unperturbed channel; d) pseudo-plug velocity  $u_{pp}(x)$ , thick horizontal line indicates the plug velocity in the unperturbed channel; (Parameters for c) & d):  $B = 5$ ,  $\delta = 0.05$ ,  $h = 0.01$ ).

same examples as in Fig. 3. We see from Figs. 3 & 4 that the pseudo-plug speed and pseudo-yield surface position essentially follow the channel width variation. The pressure gradient adjusts to force the unit flow rate through the narrower parts of the channel. In turn this results in a narrower pseudo-plug.

### 3.3 Higher order corrections: determining the true yield surface

The leading order outer solution suggests two things. First, if there is a true plug region, we might expect that the true yield surface, say  $y_T(x)$ , lies within  $O(\delta)$  of the pseudo-yield surface,  $y_y(x)$ , at each  $x$ , i.e. since this is the region

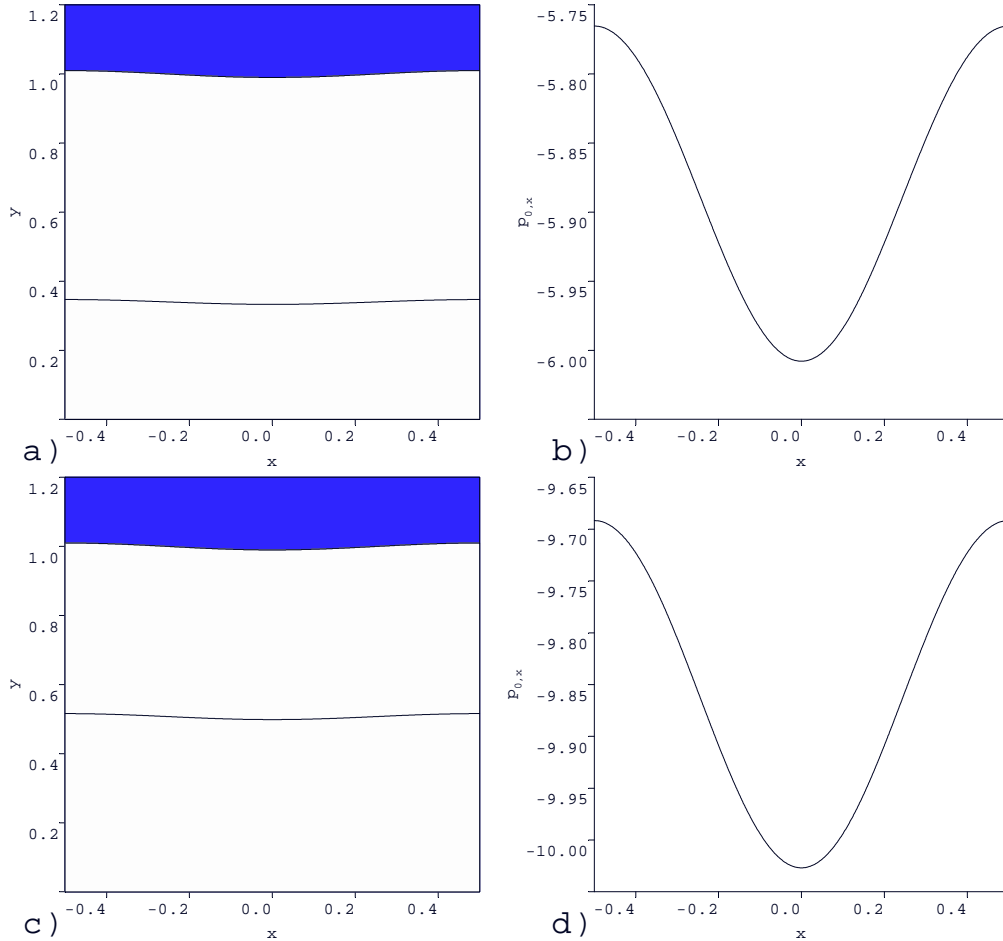


Fig. 4. The leading order outer solution: pseudo-yield surface position and pressure gradient along the channel: a)  $y_y(x)$  for parameters  $B = 2$ ,  $\delta = 0.05$ ,  $h = 0.01$ , the shaded area denotes the upper channel wall; b)  $p_{0,x}(x)$  for parameters  $B = 2$ ,  $\delta = 0.05$ ,  $h = 0.01$ ; c)  $y_y(x)$  for parameters  $B = 5$ ,  $\delta = 0.05$ ,  $h = 0.01$ ; d)  $p_{0,x}(x)$  for parameters  $B = 5$ ,  $\delta = 0.05$ ,  $h = 0.01$ .

where the leading order outer solution breaks down. Second, we might expect that the velocity of the true plug, say  $u_p$ , lies somewhere within the range of the pseudo-plug velocities, i.e.

$$u_p = u_{pp}(x_p) : \quad x_p \in [-1/2, 1/2]. \quad (33)$$

With these assumptions, we shall proceed to derive higher order corrections to  $u_0$  and complete our asymptotic solution. However, first we consider intuitively what the solution and yield surface must look like, in order for a true plug to remain along the channel length.

Suppose that  $x_p > 0$ , ( $u_{pp}(x_p) = u_{pp}(-x_p)$ , via symmetry), and consider the velocity at a fixed  $x$ , for which  $u_{pp}(x) > u_p$ , (i.e.  $|x| < x_p$ ). In this case, it is clear that the outer solution  $u_0$  is travelling essentially *too fast* along the channel centre, in the pseudo-plug. However,  $u_0$  satisfies the flow rate

constraint (28), and our corrected solution must also have the same flow rate. Thus, the  $O(\delta)$  flow rate discrepancy,  $\sim [u_{pp}(x) - u_p]y_y$ , must somehow be added via the first order velocity correction,  $u_1$ , in the outer sheared layer. Physically, we still expect the maximal velocity to be in the channel centre, at the true plug. Therefore, (and perhaps counter-intuitively), to conserve the unit areal flux through the channel, it will be necessary that the true plug is wider than the pseudo-plug at all such points,  $|x| < x_p$ . Similarly, if we consider  $x_p < |x| \leq 1/2$ , so that  $u_{pp}(x) < u_p$ , we would expect the true plug to be narrower than the pseudo-plug, since the flow rate in the outer layer must be reduced at first order. We consider these two cases separately below. We deal later, in §3.4, with determination of  $u_p$ .

### 3.3.1 The case $u_{pp}(x) < u_p$ , $y_T(x) < y_y(x)$

Here we assume that:

$$y_y(x) \sim y_T(x) + \delta\xi_T(x) + O(\delta^2), \quad (34)$$

and shall find an expression for  $\xi_T(x)$ , the first order perturbation from  $y_y(x)$ . We match our two outer velocity solutions in a transition layer of  $O(\delta)$ , by assuming a composite solution of form:

$$u \sim \begin{cases} u_p & 0 \leq y \leq y_T, \\ u_p + \delta^2 u_2^i(x, y) + \dots & y_T < y \leq y_y, \\ u_0(x, y) + \delta u_1(x, y) + \delta^2 u_2(x, y) + \dots & y_y < y \leq y_w. \end{cases} \quad (35)$$

We begin by constructing the outer solutions  $u_1$  and  $u_2$ , by defining  $u_1^*$ ,  $q_1$ ,  $u_2^*$  and  $q_2$  as follows:

$$u_1(y_y) \equiv u_1^*, \quad \int_{y_y}^{y_w} u_1 \, dy \equiv q_1, \quad u_2(y_y) \equiv u_2^*, \quad \int_{y_y}^{y_w} u_2 \, dy \equiv q_2.$$

Note that for given  $u_1^*$  and  $q_1$ , we can solve (26) for  $u_1$  and  $p_{1,x}$ ; similarly (27) for  $u_2$  and  $p_{2,x}$ . We find that:

$$u_1 = \frac{(y - y_w)}{(y_w - y_y)^2} \left[ u_1^*(3y - 2y_y - y_w) - 6q_1 \frac{(y - y_y)}{(y_w - y_y)} \right], \quad (36)$$

$$p_{1,x} = -\frac{12q_1}{(y_w - y_y)^3} + \frac{6u_1^*}{(y_w - y_y)^2}, \quad (37)$$

$$u_2 = \frac{(y - y_w)}{(y_w - y_y)^2} \left[ u_2^*(3y - 2y_y - y_w) - 6q_2 \frac{(y - y_y)}{(y_w - y_y)} \right], \quad (38)$$

$$p_{2,x} = -\frac{12q_2}{(y_w - y_y)^3} + \frac{6u_2^*}{(y_w - y_y)^2}, \quad (39)$$

The values  $u_1^*$  and  $q_1$  are found by matching to the first order inner expansion at  $y_y$ , and similarly for  $u_2^*$  and  $q_2$  at second order.

In the inner transition layer, we take the expansion

$$u^i = u_p + \delta^2 u_2^i(x, y) + \delta^3 u_3^i(x, y) + \dots, \quad (40)$$

and introduce the inner coordinate  $\xi$ :

$$y = y_T(x) + \delta\xi. \quad (41)$$

We substitute the expansion (40), (and equivalent ones for  $p^i$  and  $v^i$ ), into the lubrication equations, expand in powers of  $\delta$  and collect terms. The  $y$ -component of the inner velocity,  $v^i \sim O(\delta^3)$ , across this layer and hence  $v^i$  plays no part. The leading order shear stress is:

$$\tau_{xy} \sim B \operatorname{sign}(u_{2,\xi}^i) + \delta u_{2,\xi}^i + O(\delta^2), \quad (42)$$

and the momentum equations are:

$$0 = -p_{0,x} + u_{2,\xi\xi}^i, \quad (43)$$

$$0 = -p_{0,\xi}. \quad (44)$$

We therefore match  $p_{0,x}$  with the outer pressure gradient and integrate out from the true yield surface,  $\xi = 0$ , at which

$$0 = u_2^i = u_{2,\xi}^i.$$

This gives the following expression for  $u_2^i$ :

$$u_2^i = p_{0,x} \frac{\xi^2}{2} = -\frac{B}{2y_y} \xi^2 < 0. \quad (45)$$

At  $y_y$ , ( $\xi = \xi_T$ ), the velocity and stress for the inner solution are:

$$u^i(y_y) \sim u_p - \delta^2 \frac{B}{2y_y} \xi_T^2 + O(\delta^3), \quad (46)$$

$$\tau_{xy}^i(y_y) \sim -B - \delta \frac{B}{y_y} \xi_T + O(\delta^2). \quad (47)$$

whereas for the outer solution:

$$u(y_y) \sim u_{pp}(x) + \delta u_1^* + \delta^2 u_2^* + O(\delta^3), \quad (48)$$

$$\tau_{xy}(y_y) \sim -B + \delta u_{1,y}(y_y) + \delta^2 u_{2,y}(y_y) + O(\delta^3). \quad (49)$$

Thus, the first order velocity correction compensates for the discrepancy in plug speeds:

$$u_1^* = \frac{1}{\delta} [u_p - u^{pp}(x)], \quad (50)$$

and the  $O(\delta^2)$  terms in (46) and (48) yield

$$u_2^* = -\frac{B}{2y_y} \xi_T^2. \quad (51)$$

Hence,  $u_1^* > 0$  and  $u_2^* < 0$ . To find  $q_1$  and  $q_2$  we consider the total areal flux across the channel:

$$1 = \int_0^{y_w} u \, dy = \int_0^{y_y} u \, dy + \int_{y_y}^{y_w} u_0 + \delta u_1 + \delta^2 u_2 \, dy + O(\delta^3), \quad (52)$$

$$= y_y u_p + \int_{y_y}^{y_w} u_0 \, dy + \delta q_1 + \delta^2 q_2 + O(\delta^3), \quad (53)$$

$$= 1 + y_y [u_p - u_{pp}(x)] + \delta q_1 + \delta^2 q_2 + O(\delta^3). \quad (54)$$

Note that we have used the fact that (28) is satisfied for the leading order outer solution, (29). Also note that the contribution to the flux from the  $O(\delta^2)$  non-constant velocity terms, integrated across the transition layer, is felt at  $O(\delta^3)$ . Matching the orders above gives:

$$q_1 = -y_y u_1^*, \quad (55)$$

$$q_2 = 0. \quad (56)$$

Finally,  $\xi_T$  comes from matching the inner and outer stresses, at first order:

$$-\frac{B}{y_y} \xi_T = u_{1,y}(y_y).$$

The right-hand side can be expressed in terms of  $u_1^*$ , and after some algebra, we find:

$$\xi_T = \frac{u_1^*(y_y + 2y_w)}{u_{pp}}, \quad (57)$$

which is  $O(1)$  and positive, as required.

### 3.3.2 The case $u_{pp}(x) > u_p$ , $y_T(x) > y_y(x)$

Here we adopt a similar approach to the previous section. We expect that  $y_T(x) > y_y(x)$  and hence write

$$y_T(x) \sim y_y(x) + \delta \xi_T(x) + O(\delta^2), \quad (58)$$

We adopt the following structure for our velocity solution:

$$u \sim \begin{cases} u_p & 0 \leq y \leq y_T, \\ u_0(y_w(x), y) + \delta u_1(x, y) + \delta^2 u_2(x, y) & y_T < y \leq y_w, \end{cases} \quad (59)$$

and will choose  $u_1$  and  $u_2$  to match the velocity and stress at the yield surface, and the pressure gradients chosen so that the flux constraint is satisfied along the channel. We define  $u_1^*$ ,  $q_1$ ,  $u_2^*$  and  $q_2$  as follows:

$$u_1(y_T) \equiv u_1^*, \quad \int_{y_T}^{y_w} u_1 \, dy \equiv q_1, \quad , u_2(y_T) \equiv u_2^*, \quad \int_{y_T}^{y_w} u_2 \, dy \equiv q_2.$$

As before, in terms of  $u_1^*$ ,  $q_1$ ,  $u_2^*$  and  $q_2$  we find:

$$u_1 = \frac{(y - y_w)}{(y_w - y_T)^2} \left[ u_1^*(3y - 2y_T - y_w) - 6q_1 \frac{(y - y_T)}{(y_w - y_T)} \right], \quad (60)$$

$$p_{1,x} = -\frac{12q_1}{(y_w - y_T)^3} + \frac{6u_1^*}{(y_w - y_T)^2}, \quad (61)$$

$$u_2 = \frac{(y - y_w)}{(y_w - y_T)^2} \left[ u_2^*(3y - 2y_T - y_w) - 6q_2 \frac{(y - y_T)}{(y_w - y_T)} \right], \quad (62)$$

$$p_{2,x} = -\frac{12q_2}{(y_w - y_T)^3} + \frac{6u_2^*}{(y_w - y_T)^2}, \quad (63)$$

In order to have continuity of velocity at  $y_T$  we require

$$u_p = u_0(y_T) + \delta u_1^* + \delta^2 u_2^*,$$

which leads to:

$$u_1^* = \frac{1}{\delta} (u_p - u_{pp}(x)), \quad u_2^* = \frac{1}{\delta^2} (u_{pp}(x) - u_0(y_T(x))). \quad (64)$$

Note that both  $u_1^*$  &  $u_2^*$  are  $O(1)$  provided that  $y_T - y_y = O(\delta)$ , and that  $u_1^* < 0$ ,  $u_2^* > 0$ . Considering the flow rate through the channel, as in the previous section:

$$1 = \int_0^{y_w} u \, dy = \int_0^{y_T} u \, dy + \int_{y_T}^{y_w} u \, dy = y_T u_p + \int_{y_T}^{y_w} u_0 \, dy + \delta q_1 + \delta^2 q_2 + O(\delta^3). \quad (65)$$

From (28), we have

$$1 = y_y u_{pp} + \int_{y_y}^{y_w} u_0 \, dy,$$

and hence combining:

$$0 = [u_p - u_{pp}]y_y + \delta q_1 + [u_p - u_{pp}][y_T - y_y] + \delta q_2 + O(\delta^3). \quad (66)$$

Therefore,

$$q_1 = -y_y u_1^*, \quad q_2 = -\xi_T u_1^*. \quad (67)$$

Now  $\xi_T$  is found by matching the shear stress to  $O(\delta)$  at  $y_T$ . This requires that

$$0 = \frac{2\xi_T u_{pp}}{(y_w - y_y)^2} + \frac{2u_1^*(y_y + 2y_w + 2\delta\xi_T)}{(y_w - y_y - \delta\xi_T)^2}. \quad (68)$$

After some algebra, we find:

$$\xi_T = -\frac{u_1^*(y_y + 2y_w)}{u_{pp}}, \quad (69)$$

which is  $O(1)$  and positive, as required. The solution is complete provided that the true plug speed may be determined.

### 3.4 Determination of the true plug speed

We note that our asymptotic solutions depend only upon the plug speed,  $u_p$ , which we have assumed lies in the range of pseudo-plug speeds,  $u_{pp}(x)$ . It remains to determine the correct plug speed from this range. Within the true plug, the deviatoric stress is indeterminate, but the momentum equations are satisfied. We rewrite the  $x$ -momentum equation (8) as:

$$\frac{\partial J_1}{\partial x} - \frac{\partial J_2}{\partial y} = 0,$$

where

$$J_1 \equiv -p + \delta^2 \tau_{xx} - \delta Re u^2, \quad (70)$$

$$J_2 \equiv -\tau_{xy} + \delta Re uv. \quad (71)$$

We shall consider the integral of  $J_1(x, y)$ , between  $y = 0$  and  $y = y_T$  at a fixed arbitrary position  $x = x_b$ . By use of Green's theorem and integrating around the two contours indicated in Fig. 5, we derive the following two expressions for this integral:

$$\begin{aligned} \int_0^{y_T(x_b)} J_1(x_b, y) \, dy &= \int_0^{x_b} [J_2(x, y_T(x)) - J_2(x, 0) + y'_T(x) J_1(x, y_T(x))] \, dx \\ &\quad + \int_0^{y_T(0)} J_1(0, y) \, dy, \end{aligned} \quad (72)$$

$$\begin{aligned} \int_0^{y_T(x_b)} J_1(x_b, y) \, dy &= \int_{1/2}^{x_b} [J_2(x, y_T(x)) - J_2(x, 0) + y'_T(x) J_1(x, y_T(x))] \, dx \\ &\quad + \int_0^{y_T(1/2)} J_1(1/2, y) \, dy. \end{aligned} \quad (73)$$

The above two expressions must clearly be equal, i.e. the stress is indeterminate, but is still a single valued function of  $(x, y)$ .

Although the stresses are in general indeterminate within the plug region, we have assumed symmetry of the flow with respect to  $y = 0$ , and periodicity of our solution along the channel. Thus, we have that:

$$\tau_{xy}(x, 0) = 0, \quad v(x, 0) = 0,$$

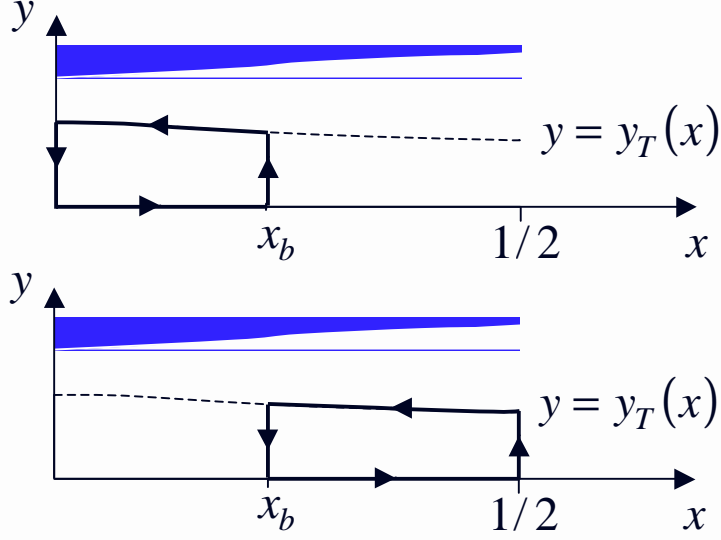


Fig. 5. Contours selected for the evaluation of (72) & (73).

and at the maxima and minima of  $y_w(x)$ , we will have

$$\tau_{xx}(\pm j/2, y) = \frac{\partial \tau_{xy}}{\partial x}(\pm j/2, y) = 0, \quad j = 0, 1, 2, 3, \dots \quad (74)$$

(see also our later discussion of the case  $h = O(1)$ , in §4). Thus, the  $y$ -momentum equation, at the maxima and minima of  $y_w(x)$ , becomes simply:

$$\frac{\partial p}{\partial y}(\pm j/2, y) = 0, \quad j = 0, 1, 2, 3, \dots,$$

Equating (72) and (72), and using the above symmetry conditions, we have:

$$\begin{aligned} 0 &= \int_0^{1/2} J_2(x, y_T(x)) + y_T'(x)[J_1(x, y_T(x))] dx + \int_0^{y_T(0)} J_1(0, y) dy \\ &\quad - \int_0^{y_T(1/2)} J_1(1/2, y) dy \\ &= \int_0^{1/2} -\tau_{xy}(x, y_T(x)) + y_T'(x)[-p + \delta^2 \tau_{xx} - \delta Re u^2](x, y_T(x)) dx \\ &\quad + \int_0^{y_T(0)} [-p - \delta Re u^2](0, y) dy - \int_0^{y_T(1/2)} [-p - \delta Re u^2](1/2, y) dy \end{aligned} \quad (75)$$

Any legitimate choice of  $u_p$  must satisfy (75). We integrate by parts the term multiplied by  $y_T'(x)$ , cancelling out the integrals at  $x = 0$ ,  $x = 1/2$ . This gives:

$$0 = \int_0^{1/2} -\tau_{xy}(x, y_T(x)) + y_T(x) \left[ \frac{\partial p}{\partial x}(x) - \delta^2 \frac{\partial}{\partial x} \tau_{xx}(x, y_T(x)) \right] dx, \quad (76)$$

note that  $u$  is independent of  $x$  along  $y = y_T$ , and is constant within the true plug. We now substitute our asymptotic solutions in the above integral and retain the leading order terms, which are of  $O(\delta)$ :

$$0 = \int_0^{1/2} [y_T(x) - y_y(x)] \frac{\partial p_0}{\partial x}(x) + \delta y_T(x) \frac{\partial p_1}{\partial x}(x) dx, \quad (77)$$

Equation (77) corresponds to a force balance. The net force of the zero-th order pressure gradient, acting on the plug perturbation, and the first order pressure gradient, acting on the full plug, should be zero, i.e. in equilibrium.

The right-hand side of (77) will depend on our choice of  $x_p$ . We define

$$F(x_p) \equiv \int_0^{1/2} [y_T(x) - y_y(x)] \frac{\partial p_0}{\partial x}(x) + \delta y_T(x) \frac{\partial p_1}{\partial x}(x) dx,$$

where  $y_T(x)$ ,  $y_y(x)$ ,  $p_{0,x}$  &  $p_{1,x}$  are functions of  $x_p$ , (i.e.  $u_p$ ), defined via the asymptotic solutions of §3.3.1 & §3.3.2. Note that if we choose the plug speed such that  $x_p = 0$ , we will have  $u_p > u_{pp}(x)$ ,  $y_T(x) < y_y(x)$ ,  $u_1^* > 0$ ,  $q_1 < 0$  and  $p_{1,x} > 0$ , at each  $x$ , (see §3.3.1). Consequently,  $F(x_p) > 0$  at  $x_p = 0$ . Conversely, selecting the widest part of the channel,  $x_p = \pm 1/2$ , we will have  $u_p < u_{pp}(x)$ ,  $y_T(x) > y_y(x)$ ,  $u_1^* < 0$ ,  $q_1 > 0$  and  $p_{1,x} < 0$ , at each  $x$ , and therefore  $F(x_p) < 0$  at  $x_p = 0.5$ , (see §3.3.2). Thus, there is at least one value of  $x_p$ , (or  $u_p$ ), for which the above integral vanishes. In fact we may generally expect the variation in  $F(x_p)$  to be strictly monotone for  $x_p \in (0, 1/2)$ , and thus the equation

$$0 = F(x_p), \quad (78)$$

uniquely determines the plug speed. Two examples of  $F(x_p)$  are shown in Fig. 6. It can be seen that the zero of (78) is close to  $x_p = 0.25$ , which corresponds to the plug speed in the unperturbed uniform channel.

The zero of (78) is easily computed using a bisection method. In Fig. 7 we show the variation of  $x_p$  with the parameters  $B$ ,  $\delta$  and  $h$ . Whilst departures from the plane channel plug speed are small, they are observable. Figs. 7a & b indicate that increasing  $B$  reduces  $x_p$ , which implies an increase in the true plug speed  $u_p$ . This effect is larger with larger  $\delta$  and  $h$ , as is to be expected. Also interesting is that at large  $B$ , it appears that  $x_p$  approaches some limit.

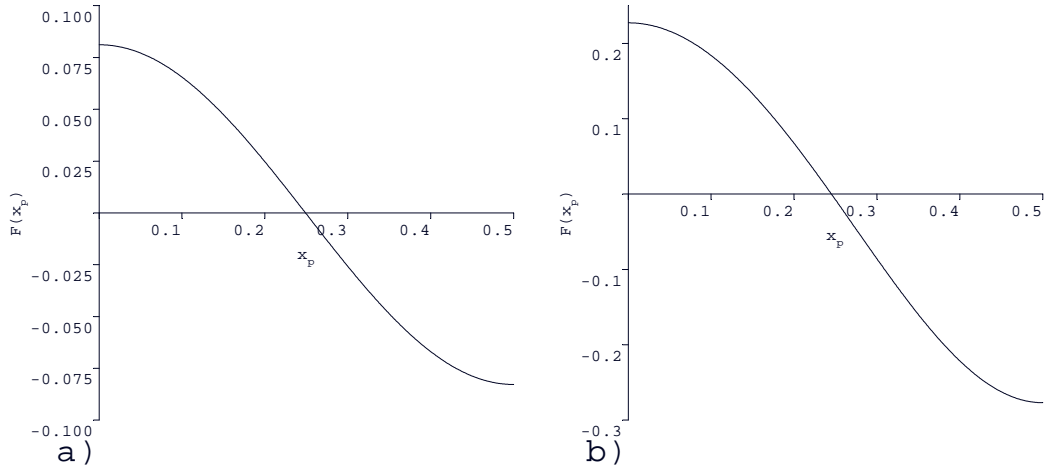


Fig. 6. The function  $F(x_p)$ : a) parameters  $B = 2$ ,  $\delta = 0.05$ ,  $h = 0.01$ ; b) parameters  $B = 5$ ,  $\delta = 0.05$ ,  $h = 0.01$ .

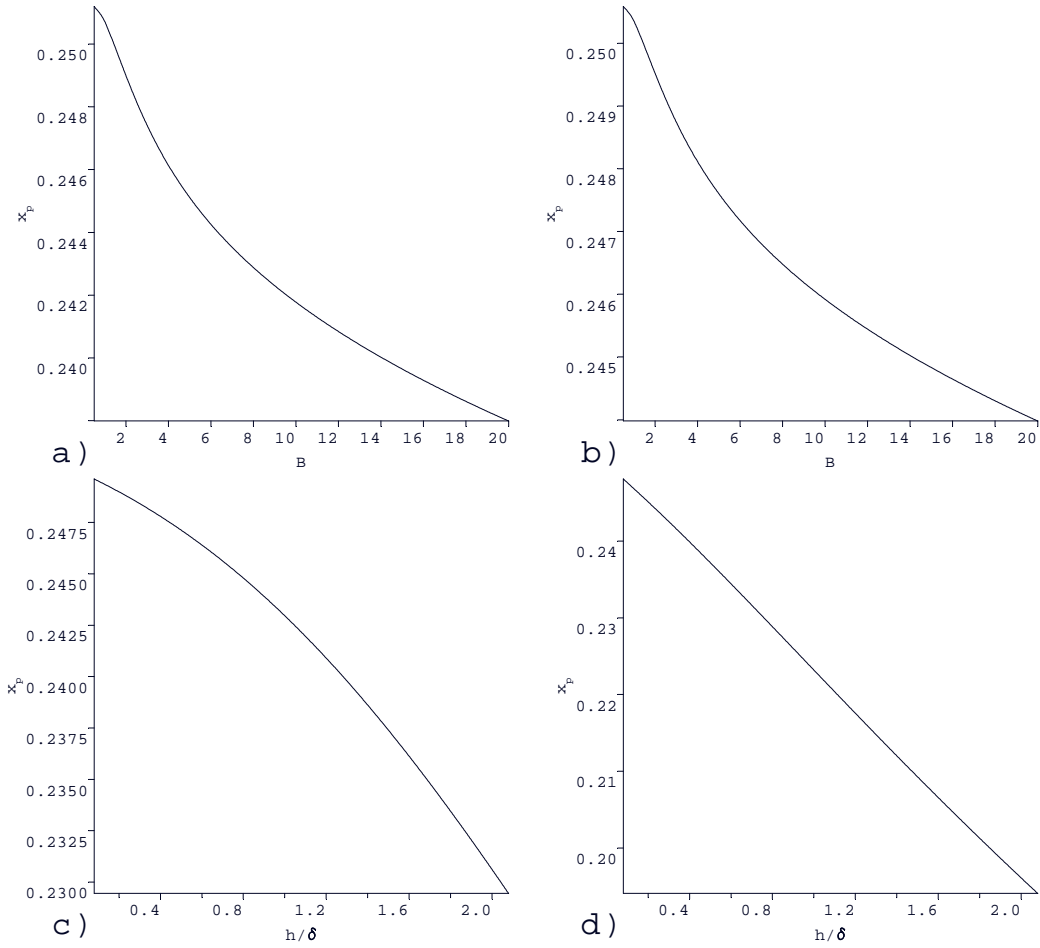


Fig. 7. Variations in  $x_p$  with  $B$ ,  $\delta$  and  $h$ : a)  $\delta = 0.05$ ,  $h = 0.01$ , variation with  $B$ ; b)  $\delta = 0.02$ ,  $h = 0.005$ , variation with  $B$ ; c)  $B = 2$ ,  $\delta = 0.05$ , variation with  $h/\delta$ ; d)  $B = 5$ ,  $\delta = 0.05$ , variation with  $h/\delta$ .

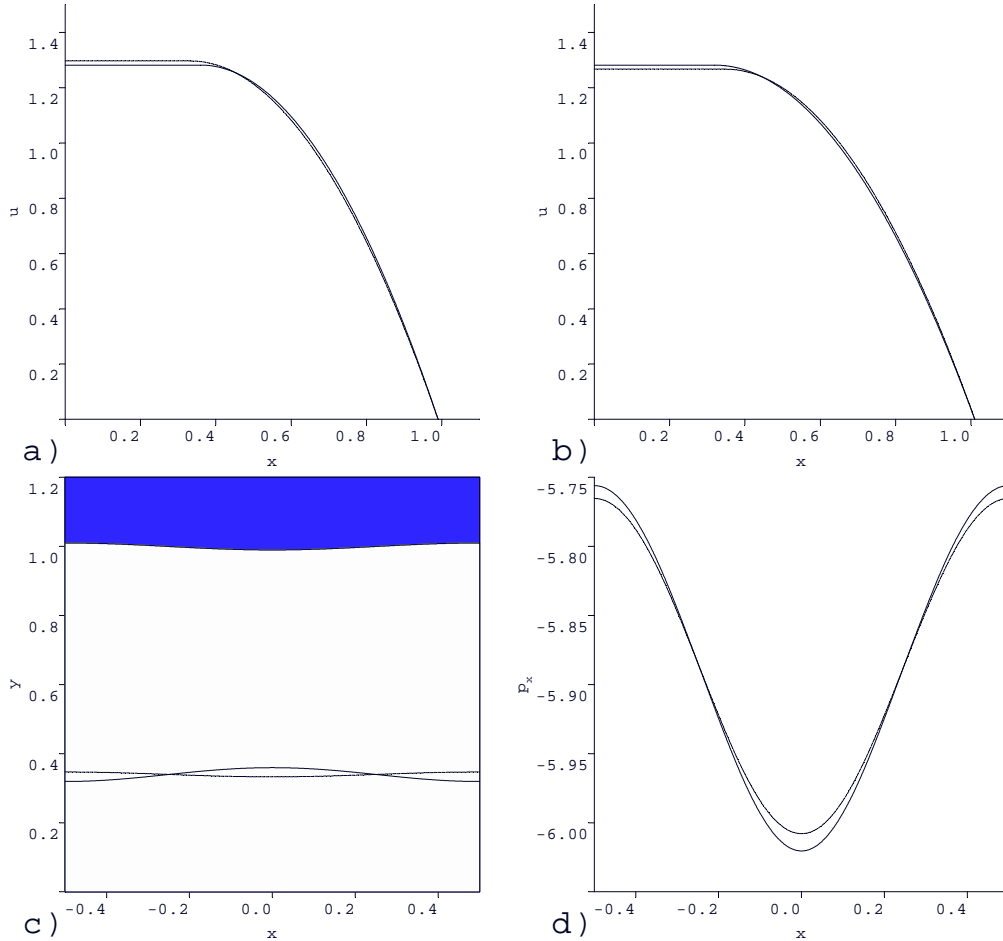


Fig. 8. Composite asymptotic solutions, (thick line), compared with the zero-th order outer approximation for  $B = 2$ ,  $\delta = 0.05$ ,  $h = 0.01$ : a) velocity solution at  $x = 0$ ; b) velocity solution at  $x = 0.5$ ; c) true yield surface  $y_T(x)$ , (thick line), and pseudo-yield surface,  $y_y(x)$ , (thin line); d) composite pressure gradient,  $p_{0,x} + \delta p_{1,x}$ , (thick line), and zero-th order approximation,  $p_{0,x}$ .

If  $B$  and  $\delta$  are fixed then the amplitude  $h$  determines the plug speed,  $u_p$ . As the ratio  $h/\delta$  increases we observe a nearly linear decrease in  $x_p$ , (hence an increase in  $u_p$ ), see Fig. 7c. This effect is amplified by large  $B$ , see Fig. 7d.

### 3.5 Example solutions

We present examples of our composite asymptotic solutions, in Figs. 8 & 9. We show the corrected velocity compared against the zero-th order approximation  $u_0(y, y_w(x))$ , at the widest and narrowest parts of the channel,  $x = 0$  and  $x = 1/2$ . The difference in velocity is barely discernible in each case.

In contrast, the difference in yield surface position,  $y_T(x)$ , (Figs. 8c & 9c), from the pseudo-yield surface,  $y_y(x)$ , is quite visible. Furthermore, the yield surface variation with  $x$  is in the opposite sense to that of the pseudo-yield surface.

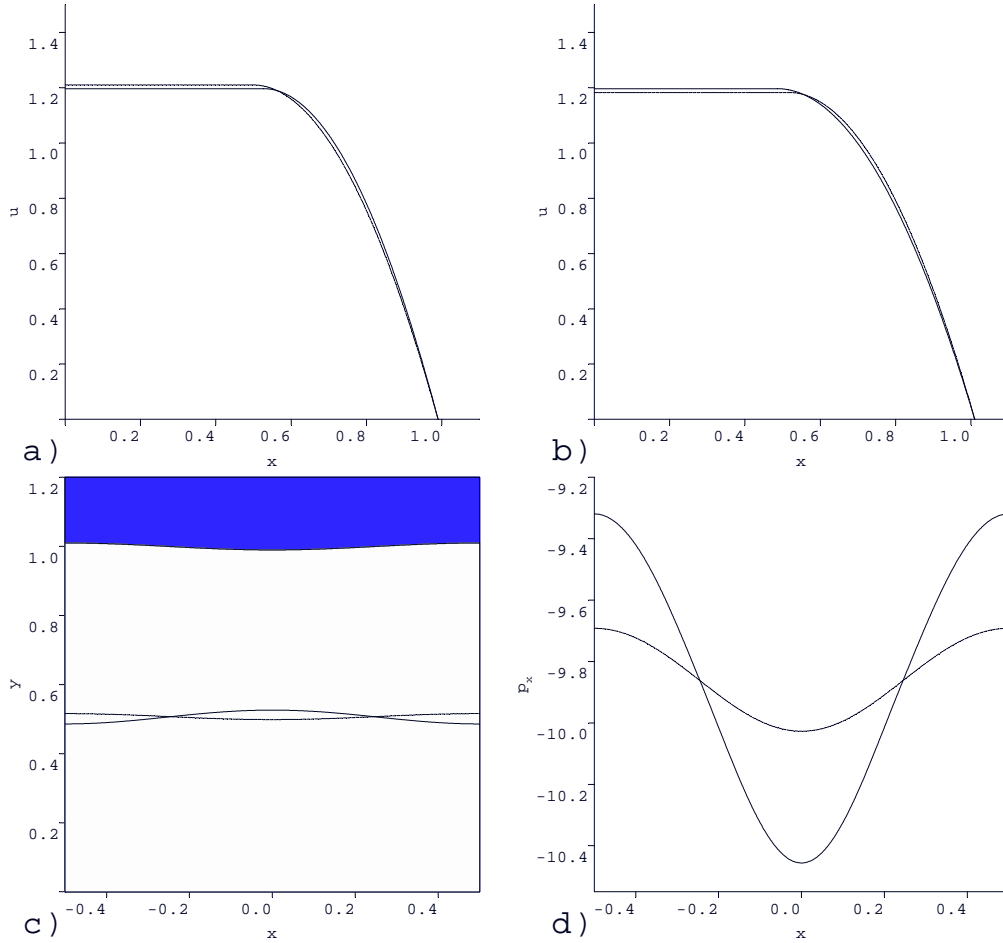


Fig. 9. Composite asymptotic solutions, (thick line), compared with the zero-th order outer approximation for  $B = 5$ ,  $\delta = 0.05$ ,  $h = 0.01$ : a) velocity solution at  $x = 0$ ; b) velocity solution at  $x = 0.5$ ; c) true yield surface  $y_T(x)$ , (thick line), and pseudo-yield surface,  $y_y(x)$ , (thin line); d) composite pressure gradient,  $p_{0,x} + \delta p_{1,x}$ , (thick line), and zero-th order approximation,  $p_{0,x}$ .

Although this may appear counter-intuitive, it follows as a consequence of mass conservation and of having an intact plug. For example, with an intermediate plug velocity  $u_p$  determined, (see §3.4), the plug velocity will be slower than that of the *natural* velocity profile,  $u_{pp}(x)$  at  $x = 0$ . In order to achieve the same flow rate through the channel, it is necessary to both increase the true plug width and to augment the flow outside of the true plug. The latter is only achieved by having  $p_{1,x}(0) < 0$ .

In line with the above argument, we see that the magnitude of the pressure gradient,  $p_x(x) \sim p_{0,x}(x) + \delta p_{1,x}(x)$ , is increased in the narrow parts of the channel, see Figs. 8d & 9d. The pressure gradient perturbation,  $\delta p_{1,x}(x)$ , acts to accelerate the yielded part of the flow where  $|x| < x_p$ , and to decelerate the yielded part of the flow where  $|x| > x_p$ . We see that the size of the perturbation is significant and increases with  $B$ .

### 3.6 Effects of inertia: $Re \sim O(1)$

Although we have ignored inertia, we may readily see that even if  $Re \sim O(1)$ , inertia does not play a large role for  $h = O(\delta)$ . Reviewing the procedure in §3.3.1 & §3.3.2, for our asymptotic solutions, we see that inclusion of inertia will affect only the second order terms. The position of the true yield surface and the selection of the plug speed are determined at first order and hence there is no effect of inertia on these.

For  $Re \sim O(1)$ , the second order velocity profile  $u_2$  and the pressure gradient correction  $p_{2,x}$ , satisfy:

$$Re \frac{[u_0 u_{0,x} + v_0 u_{0,y}]}{\delta} = -p_{2,x} + u_{2,yy}, \quad (79)$$

with boundary and flux conditions:

$$\text{\S 3.3.1 :} \quad u_2(y_y) = u_2^*, \quad u_2(y_w) = 0, \quad \int_{y_y}^{y_w} u_2 \, dy = q_2, \quad (80)$$

$$\text{\S 3.3.2 :} \quad u_2(y_T) = u_2^*, \quad u_2(y_w) = 0, \quad \int_{y_T}^{y_w} u_2 \, dy = q_2. \quad (81)$$

The values of  $u_2^*$  and  $q_2$  are obtained from the same matching conditions as previously in §3.3.1 & §3.3.2. Thus, we see that inertia acts simply as a localised momentum source in (79). We have not explored these effects further.

## 4 Breaking the unyielded plug

Here we shall assume that there exists a critical amplitude  $h = h_c$  at which the true plug is no longer able to remain intact, and we shall estimate  $h_c$ . The method that we use is adapted from the work of Szabo & Hassager, on flow in an eccentric annulus, [3]. We assume that our composite asymptotic solution of the previous section is valid for  $h \sim O(\delta)$ , provided that the relative amplitude  $h/\delta$  is sufficiently small. As we approach the plug from outside, we therefore know that  $\tau_{xy} \sim -B$  and  $\tau_{xx} \sim O(\delta)$ . Within the true plug, the shear stresses are indeterminate.

If the plug breaks, a new asymptotic solution is possible within the broken plug, (see §4.1, following [19]), and that  $\tau_{xx} \sim O(\delta^{-1})$  in the extensional flow that represents the broken plug. Note that with the lubrication scaling, this

simply means that the extensional stress is of the same size as the shear stress, as is intuitive. This suggests that within the true plug, at an amplitude  $h$  close to  $h_c$ , the shear stresses are distributed such that  $\tau_{xx} \sim O(\delta^{-1})$ , within the true plug, but that  $\tau_{xx} \rightarrow O(\delta)$  at the true yield surface.

We use Green's theorem, as before, to find an expression for the integral of the extensional stress,  $\tau_{xx}$ , along a line between  $y = 0$  and  $y = y_T$ , at a fixed point  $x = x_b$ . Although  $\tau_{xx}$  is indeterminate, this procedure gives an estimate for the mean extensional shear stress across the plug at a potential breaking point,  $x_b$ . When this exceeds the yield stress, we may conclude that the plug has broken.

For given  $x_b \in [0, 1/2]$ , we define the stress integral  $I(x_b)$  by:

$$I(x_b) \equiv \delta \int_0^{y_T(x_b)} \tau_{xx}(x_b, y) dy. \quad (82)$$

A sufficient condition for the plug to have broken, (somewhere within the true plug), at point  $x = x_b$  is that

$$|I(x_b)| > B y_T(x_b). \quad (83)$$

Integrating the  $x$ -momentum equation over the contour in Fig. 5a, and using Green's theorem, we have:

$$\begin{aligned} \delta I(x_b) = & \int_0^{y_T(x_b)} [p + Re\delta u^2] dy - \int_0^{y_T(0)} [p + Re\delta u^2] dy - \\ & \int_0^{x_b} \tau_{xy}(x, y_T) + y'_T [p(x, y_T) - \delta^2 \tau_{xx}(x, y_T) + Re\delta u^2(x, y_T)] dx. \end{aligned} \quad (84)$$

(see also (72) and following). We suppose that the left-hand side of (84) will be  $O(\delta)$  if  $h$  is close to  $h_c$ , and accordingly we expand the right-hand side (84) to  $O(\delta)$ . The term  $\delta^2 \tau_{xx}(x, y_T) \sim O(\delta^3)$  and is neglected. We also have that  $\tau_{xy}(x, y_T) \sim -B + O(\delta^2) = p_{0,x} y_y(x) + O(\delta^2)$ . The inertial terms in the third integral are integrated by parts and cancel with those in the first two integrals. We finally integrate by parts the pressure term. We find:

$$I(x_b) = \int_0^{x_b} p_{0,x}(x) \frac{[y_T(x) - y_y(x)]}{\delta} + p_{1,x}(x) y_T(x) dx + O(\delta), \quad (85)$$

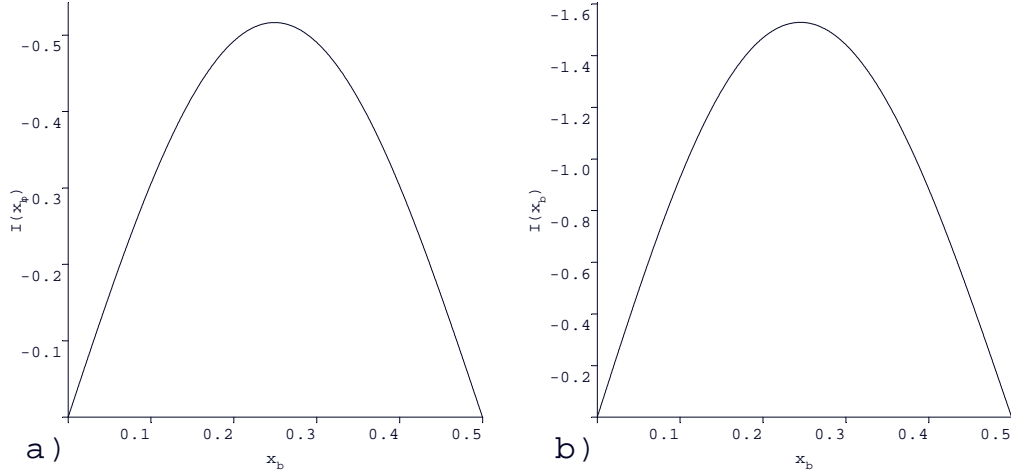


Fig. 10. The function  $I(x_b)$ : a) parameters  $B = 2$ ,  $\delta = 0.05$ ,  $h = 0.01$ ; b) parameters  $B = 5$ ,  $\delta = 0.05$ ,  $h = 0.01$ .

i.e.  $I(x_b)$  is the force that results from the action of the zero-th order pressure gradient, acting on the plug perturbation, and the first order pressure gradient acting on the entire plug. In Fig. 10 we show plots of  $I(x_b)$ , for two different choices of  $(B, h, \delta)$ . These plots are qualitatively typical, in that  $I(x_b)$  has a single minima and that  $I(x_b) = 0$  at  $x_b = 0$  and  $x_b = 0.5$ . In fact, the latter follows automatically from the definition of  $x_p$ , (see in §3.4).

Our condition (83), will be met at the minima of  $I(x_b)$ . Differentiating (85), we see that the minimum is when

$$p_{0,x}(x_b) \frac{[y_T(x_b) - y_y(x_b)]}{\delta} + p_{1,x}(x_b) y_T(x_p) = 0, \quad (86)$$

which occurs when  $y_T(x_b) = y_y(x_b)$  and  $p_{1,x}(x_b) = 0$ , i.e. when the zero-th order outer solution coincides with the corrected solution, which occurs only at  $x_b = x_p$ . This is confirmed numerically.

Therefore, we have the interesting result that the position at which the true plug will break is given by  $x_b = x_p$ . At this point  $y_T(x_b) = y_y(x_b)$  and hence the criteria for the plug to break is:

$$\left| \int_0^{x_p} p_{0,x}(x) \frac{[y_T(x) - y_y(x)]}{\delta} + p_{1,x}(x) y_T(x) \, dx \right| > B y_y(x_b). \quad (87)$$

For fixed  $(B, \delta)$ , the right-hand side of (87) will not vary with the amplitude  $h$ , whereas the left-hand side will increase with amplitude. Therefore, there exists a critical amplitude  $h_c$  at which the plug will break. This is found numerically, in a straightforward manner.

In Fig. 11 we plot the ratio  $h_c/\delta$  for  $\delta = 0.0001, 0.001, 0.01, 0.05, 0.1$ . The

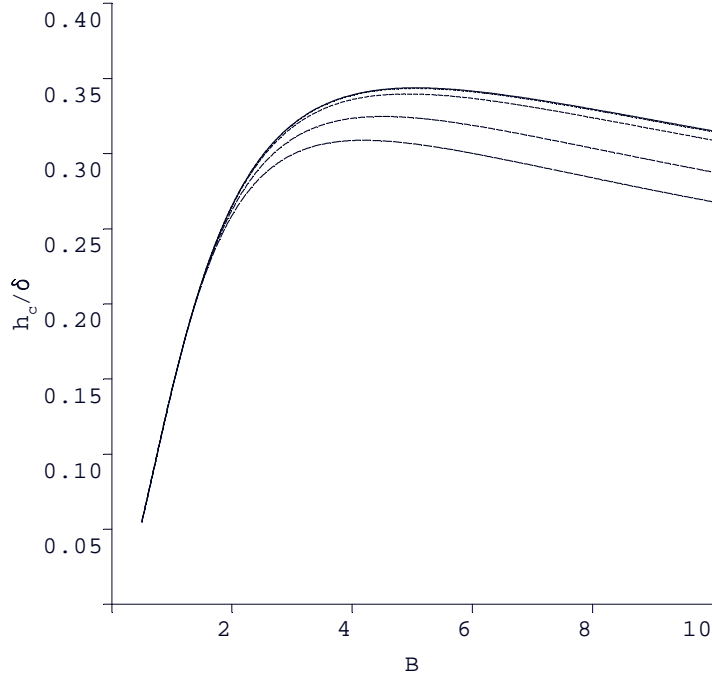


Fig. 11. The critical breaking amplitude  $h_c$ , as a function of  $(B, \delta)$ . Plotted is  $h_c/\delta$  for  $\delta = 0.0001, 0.001, 0.01, 0.05, 0.1$ ; the curves  $h_c/\delta(B)$  decrease with  $\delta$ .

ratio  $h_c/\delta$  decreases very slightly with increasing  $\delta$ . The curves for the two smallest values are indistinguishable and approximately indicate the asymptotic limit. This in itself is interesting. What is also interesting in Fig. 11 is that there is a maximum in the curve  $h_c/\delta(B)$ , which occurs at  $B \approx 5$ .

Physically, we might explain this as follows. For small  $B$  the plug region is narrower and is less able to withstand a perturbation of the channel width, i.e. since the yield stress is small. However, for large  $B$  the plug region is large and limits the width of the yielded fluid layer. It is the yielded layer which must compensate for the variations in true plug width away from the pseudo-plug width. It does this via the first order perturbation  $(u_1, p_{1,x})$ . For large  $B$  the pressure gradient perturbation becomes increasingly large, and this contributes to the left-hand side of (87), eventually causing the plug to break. Thus, the yield stress plays a dual role in maintaining/breaking the plug, and the maximal ratio of  $h_c/\delta$  is found at an intermediate Bingham number.

It is clear that  $h = h_c$  determines an upper limit for the validity of our asymptotic solutions. We may question what happens to the solution when  $h > h_c$ . In Figs. 12 & 13 we plot the asymptotic solution for  $h = 0.02$  and  $h = 0.05$ , respectively, for parameters  $(B, \delta) = (5, 0.05)$ , (compare with Fig. 9). For these values of  $(B, \delta)$ , the critical amplitude is  $h_c \approx 0.0162$ .

We see that just above the critical amplitude, the solutions still appear phys-

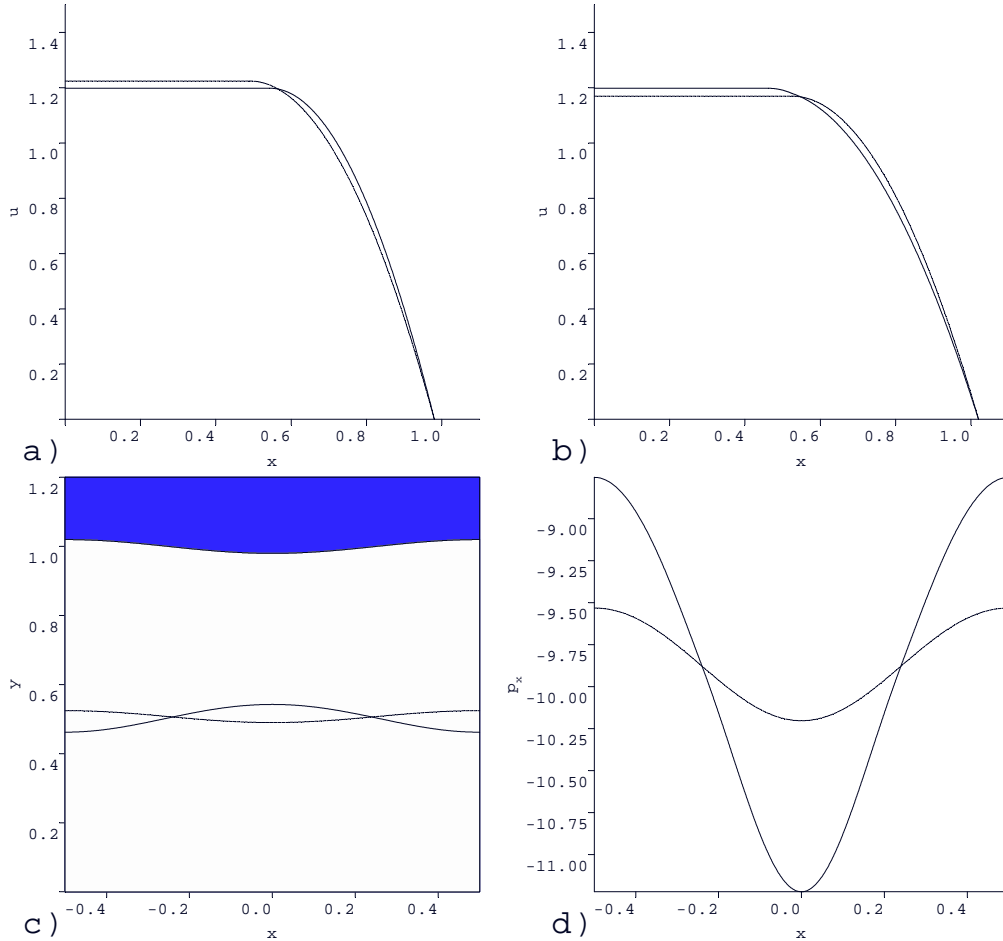


Fig. 12. Composite asymptotic solutions, (thick line), for  $h > h_c \approx 0.0162$  at parameters  $B = 5$ ,  $\delta = 0.05$ ,  $h = 0.02$ : a) velocity solution at  $x = 0$ ; b) velocity solution at  $x = 0.5$ ; c) true yield surface  $y_T(x)$ , (thick line), and pseudo-yield surface,  $y_y(x)$ , (thin line); d) composite pressure gradient,  $p_{0,x} + \delta p_{1,x}$ , (thick line), and zero-th order approximation,  $p_{0,x}$ .

ically plausible, see Fig. 12. The perturbation of the velocity appear regular and the yield surface and pressure gradient perturbations simply amplify. However, the correction to the pressure gradient,  $\delta p_{1,x}(x)$ , is becoming of the same order as the zero-th order term,  $p_{0,x}(x)$ , which suggests that the asymptotic procedure is breaking down. This is exaggerated at still higher amplitudes, see Fig. 13. At these higher amplitudes the velocity profiles also become unphysical.

In developing the solutions in §3.3.1 & §3.3.2 we have stopped at second order. These solutions are  $C^1$  at first order, (since velocity and stress are matched), but higher order terms have not been matched, (since we have truncated at second order). Thus, when the higher order terms in the perturbation become large, we see discontinuities in the gradient emerge. These occur at  $y_y$  for the solutions in §3.3.1 and at  $y_T$  for the solutions in §3.3.2. For the solutions in §3.3.1 this could be improved by a better asymptotic matching procedure,

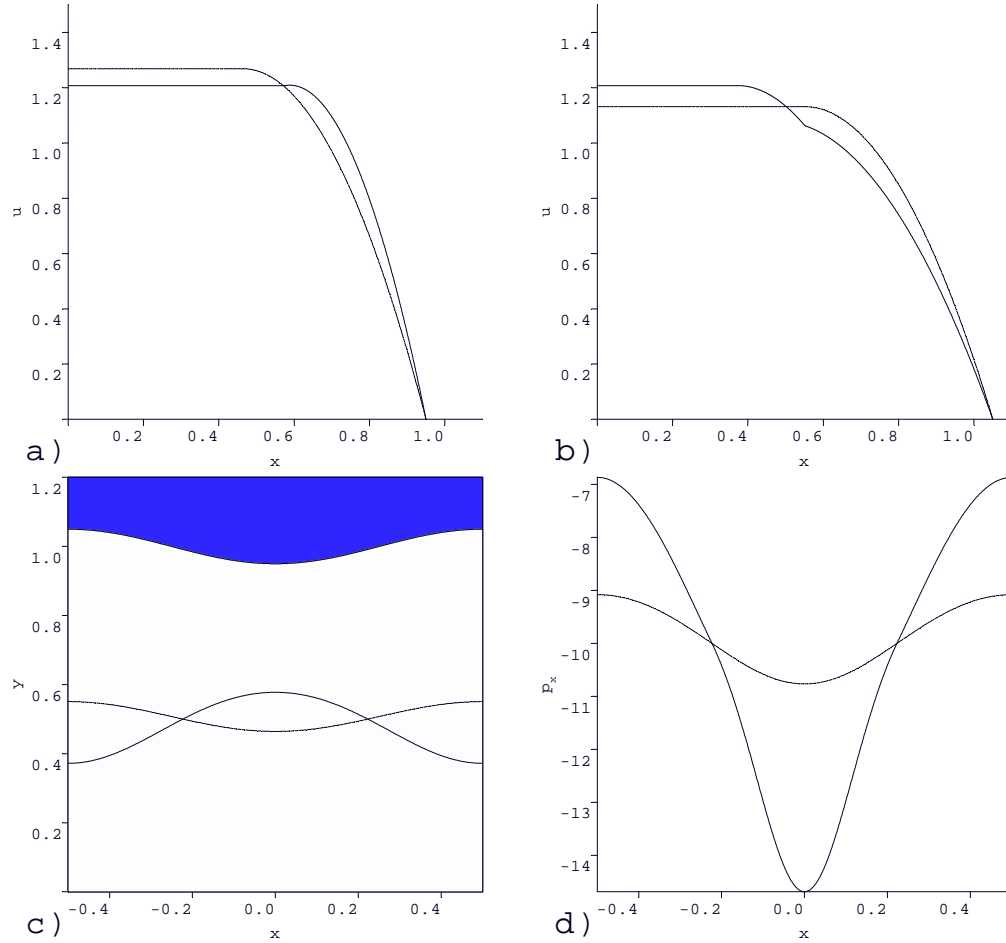


Fig. 13. Composite asymptotic solutions, (thick line), for  $h > h_c \approx 0.0162$  at parameters  $B = 5$ ,  $\delta = 0.05$ ,  $h = 0.05$ : a) velocity solution at  $x = 0$ ; b) velocity solution at  $x = 0.5$ ; c) true yield surface  $y_T(x)$ , (thick line), and pseudo-yield surface,  $y_y(x)$ , (thin line); d) composite pressure gradient,  $p_{0,x} + \delta p_{1,x}$ , (thick line), and zero-th order approximation,  $p_{0,x}$ .

(i.e. we have patched the solutions at  $y_y$ , rather than matched). However, this seems unnecessary since we have not found unphysical solutions for  $h < h_c$ .

#### 4.1 The broken plug: $h = O(1)$

We consider here the structure of the flow after the plug has broken,  $h = O(1) \gg h_c$ . For simplicity we consider  $Re \ll 1$  and hence the Stokes flow problem, where (8-9) are replaced by:

$$0 = -\frac{\partial p}{\partial x} + \delta^2 \frac{\partial}{\partial x} \tau_{xx} + \frac{\partial}{\partial y} \tau_{xy}, \quad (88)$$

$$0 = -\frac{\partial p}{\partial y} + \delta^2 \frac{\partial}{\partial x} \tau_{xy} + \delta^2 \frac{\partial}{\partial y} \tau_{yy}. \quad (89)$$

We note in passing that, in contrast to when  $h = O(\delta)$ , inertial effects will be felt at first order, and may be significant. However, this is beyond the scope of our study. The above system is similar to that analysed in [19], for thin film flow down an inclined plane.

Our focus will be on a cross-section of channel,  $x$ , at which there is no true plug region. Following [19], we expect the asymptotic solution to again consist of an outer region close to the wall, where the first approximation is that of a Poiseuille flow in a channel of width  $y_w(x)$ , another outer region in the channel centre (the pseudo-plug), where the flow is extensional, and an inner region that joins the two outer regions, close to the position of the pseudo-yield surface. The outer solution close to the wall is analogous to that developed in §3.1, and the leading order axial velocity is given by (29), which depends only on  $B$  and  $y_w(x)$ . The limiting value of the outer solution as  $y \rightarrow y_y(x)$  is again denoted  $u_{pp}(x)$ , and  $u_{pp}(x)$  is largest where the channel is narrowest and vice versa. However now, since  $h = O(1)$ , the gradient of the axial velocity,  $u_{pp,x}(x)$ , is no longer  $O(\delta)$ .

In the pseudo-plug,  $0 \leq y < y_y(x)$ , we may follow the procedure of [19] and derive the following expressions for the stress and velocity, at leading order:

$$u(x, y) \sim u_{pp}(x) + \delta \left[ 2|u_{pp,x}|(y_y^2 - y^2)^{1/2} + u_1^* \right] + O(\delta^2), \quad (90)$$

$$v(x, y) \sim -yu_{pp,x}(x) + O(\delta), \quad (91)$$

$$\tau_{xy} \sim -\frac{By}{y_y} + O(\delta) \quad (92)$$

$$\tau_{xx} \sim \frac{1}{\delta} \text{sgn}(u_{pp,x}) B \left( 1 - \frac{y^2}{y_y^2} \right)^{1/2} + O(1). \quad (93)$$

Thus, we observe that within the pseudo-plug region the leading order stress is exactly equal to the yield stress  $B$ . We can develop the series further and will find that

$$\tau \sim B + \delta \frac{\dot{\gamma}_0}{B} + O(\delta^2),$$

where  $\dot{\gamma}_0$  is the leading order rate of strain. Thus, the pseudo-plug region is a *slightly yielded* region within which the rates of strain have similar size. However, the flow is still driven by the outer shear flow. For the matching procedure at  $y_y$  and further details, we refer to [19].

A key question is whether the above solution describes the flow at each position  $x$ , along the channel, i.e. are there any fully unyielded regions that remain or is the entire channel centre one long extensional flow. The outer shear flow solution (29), (hence  $u_{pp}(x)$  also), depends solely on the channel width  $y_w(x)$

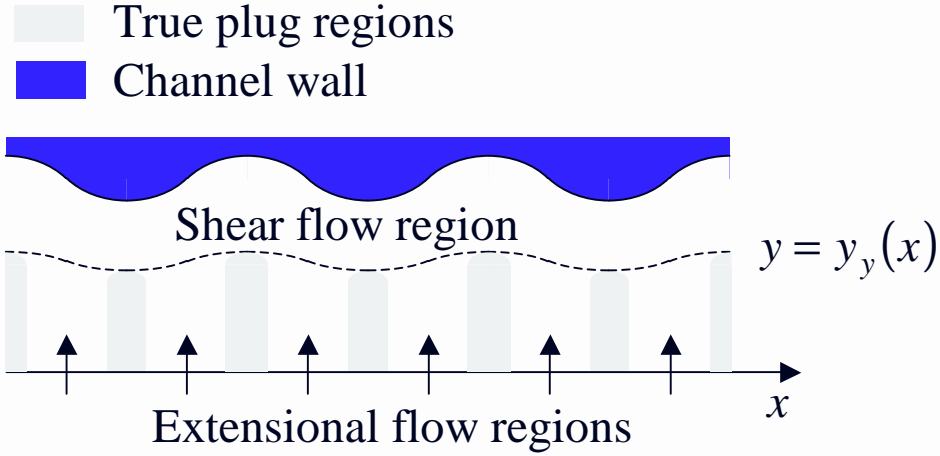


Fig. 14. Schematic of the flow structure for  $h = O(1)$ , showing the shear flow region, true plug regions at points of symmetry of  $y_w(x)$  and extensional flow regions where the analysis in [19] gives the solution.

and on  $B$ . Thus, at the extrema of  $y_w(x)$ , we have that  $u_{pp,x} = 0$ . At such points we see that  $\tau_{xx} = 0$ . Since also  $\tau_{xy} = 0$  at  $y = 0$ , we can assert that there will be fully unyielded material, (a true plug), in some region around the points  $(x, y) = (\pm n/2, 0)$ ;  $n = 0, 1, 2, \dots$ . Thus, the flow will consist of a mix of fully yielded shear flow regions, yielded pseudo-plugs and fully unyielded true plug *islands*, as shown schematically in Fig. 14.

We are unable to specify the exact shape of the true plug regions. Indeed this is one of a number of interesting problems still outstanding for slowly varying/lubrication geometries. However, expanding  $y_w(x)$  about a maxima or minima, say  $x = x_0$ :

$$y_w(x) \sim y_w(x_0) + \frac{(x - x_0)^2}{2} y_{w,xx}(x_0) + O((x - x_0)^3),$$

we see that for  $(x - x_0) \sim \delta^{1/2}$ , the variation in  $y_w(x)$  is  $O(\delta h)$ . The asymptotic method of §3.3.1 & §3.3.2 is valid for an  $O(\delta)$  variation in the channel width. Thus, presumably we could adopt this procedure here, although our procedure for finding the true plug speed needs modifying. This suggests that the true plug islands extend for an  $O(\delta^{1/2})$  width about each maxima and minima.

Note that without the asymptotic expressions, we can still infer the structure of the flow from symmetry and continuity arguments. As a Stokes flow we can demonstrate uniqueness of the velocity solution and symmetry of the streamlines about  $x = 0$ , (or indeed any of the extrema of our periodic  $y_w(x)$ ). Thus, we may infer that  $\tau_{xx}$  changes sign at each extrema of  $y_w(x)$ . Since also  $\tau_{xy} = 0$  along the  $x$ -axis, from symmetry and by continuity, we have a sequence of true plug islands surrounding the points  $(x, y) = (\pm n/2, 0)$ ;  $n = 0, 1, 2, \dots$ , at each of which,  $\tau = 0$ .

#### 4.1.1 A necessary condition for the plug to break

From the extensional flow solution (93), we observe that  $\tau_{xx} \sim O(\delta^{-1})$  in the extensional pseudo-plug, once the true plug breaks. Integrating  $\delta\tau_{xx}$  across the pseudo-plug, at a position  $x_b$ , we find that:

$$|I(x_b)| \sim \frac{\pi B y_y(x_b)}{4} + O(\delta), \quad (94)$$

for the broken plug solution. Thus,  $|I(x_b)|$  is generally smaller than  $B y_y(x_B)$ , which is our sufficient condition determining plug-breaking, (87). We infer that either: (i) once the plug has broken, the extensional stresses in the pseudo-plug are able to relax to (93), or alternatively, (ii) the condition (87) is sufficient but perhaps not necessary, to break the plug.

If we take the second interpretation, a necessary condition to break the plug follows from (94):

$$\left| \int_0^{x_p} p_{0,x}(x) \frac{[y_T(x) - y_y(x)]}{\delta} + p_{1,x}(x) y_T(x) \, dx \right| > \frac{\pi B y_y(x_p)}{4}. \quad (95)$$

In Fig. 15, we plot the necessary critical amplitude  $h_{c,n}$ , from criteria (95), for various  $(B, \delta)$ . The results are similar to Fig. 11, except that evidently  $h_{c,n} < h_c$ .

## 5 Comparison with the distinguished limit of the bi-viscous model

For completeness, we compare the results of §3 with the distinguished limit of the bi-viscous model. This asymptotic method was developed in the 1990's in a series of papers by S.D.R. Wilson, [7,20,27,28], and has been used by other authors for a range of lubrication problems, e.g. [25,26]. The method is purported to resolve the lubrication paradox, but we shall see that very different results are produced than those in §3.

In outline, the method is as follows. The lubrication scalings and equations are adopted, (identically as we have), but the constitutive laws are replaced by the following bi-viscous model:

$$\tau_{ij} = \left(1 + \frac{B(1-\epsilon)}{\dot{\gamma}}\right) \dot{\gamma}_{ij} \iff \dot{\gamma} > \epsilon B \quad (96)$$

$$\tau_{ij} = \frac{\dot{\gamma}_{ij}}{\epsilon} \iff \dot{\gamma} \leq \epsilon B. \quad (97)$$

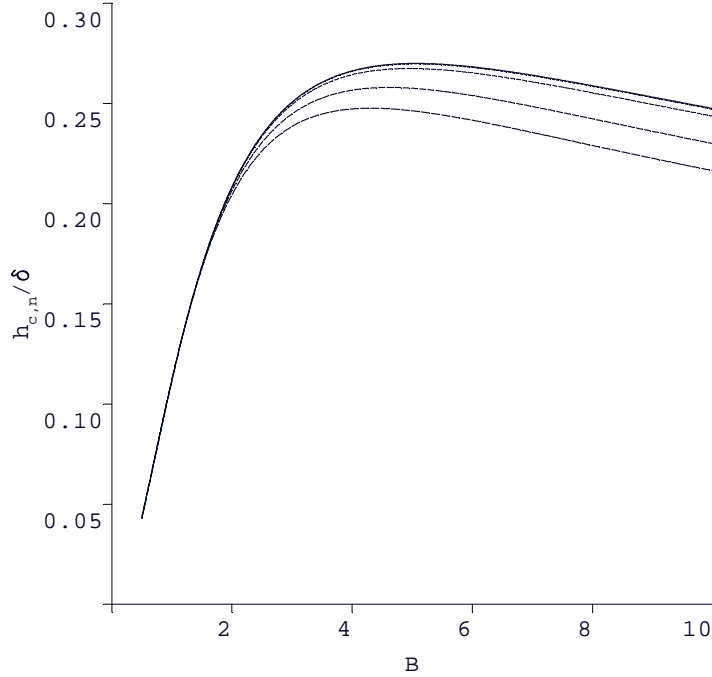


Fig. 15. The necessary condition for the critical breaking amplitude  $h_{c,n}$ , as a function of  $(B, \delta)$ . Plotted is  $h_{c,n}/\delta$  for  $\delta = 0.0001, 0.001, 0.01, 0.05, 0.1$ ; the curves  $h_{c,n}/\delta(B)$  decrease with  $\delta$ .

The parameter  $\epsilon \ll 1$  represents the ratio between the plastic viscosity in the (dimensional) Bingham model and a bi-viscous *low-shear* viscosity. Thus, the indeterminacy of the exact Bingham model is removed.

The lubrication method proceeds straightforwardly, expanding the momentum equations in powers of the two small parameters,  $\delta$  and  $\epsilon$ . It is argued that the correct asymptotic solution will be recovered as the distinguished limit:

$$\epsilon \rightarrow 0, \quad \delta \rightarrow 0, \quad \epsilon = k\delta,$$

where  $k \sim O(1)$  is fixed.

In application to the channel flow, it is assumed that there is an outer shear layer, (in which the treatment is identical to ours earlier), coupled to the pseudo-plug at  $y = y_y(x)$ . Within the pseudo-plug, we assume

$$u(x, y) \sim u_{pp}(x) + \delta u_1(x, y) + \delta^2 u_2(x, y) + \dots,$$

as before. The leading order approximation to the shear stress, within the pseudo-plug, is found to be:

$$\tau \sim \left[ \frac{B^2 y^2}{y_y^2} + 4 \frac{u_{pp,x}^2}{k^2} \right]^{1/2}. \quad (98)$$

According to this method, the true yield surface is where  $\tau = B$ , and thus we find:

$$y_{T,k} \sim y_y \left[ 1 - 4 \frac{u_{pp,x}^2}{B^2 k^2} \right]^{1/2}, \quad (99)$$

where we have appended the subscript  $k$  to distinguish from our earlier expression.

To complete the velocity solution note that for  $y \in [0, y_{T,k}(x)]$  the constitutive law is (97), whereas in the layer,  $y \in (y_{T,k}(x), y_y(x))$ , the yield stress is exceeded and the constitutive law is (96), as in the outer shear layer. The full expression for the velocity can be evaluated by careful expansion in each region. We find that:

$$u \sim u_0(x, y) + \delta u_1(x, y) + \dots \quad (100)$$

$$u_1 = \begin{cases} u_1^* + 2|u_{pp,x}|(y_y^2 - y_{T,k}^2)^{1/2} + \frac{kB}{2y_y}(y_{T,k}^2 - y^2) & y \in [0, y_{T,k}], \\ u_1^* + 2|u_{pp,x}|(y_y^2 - y^2)^{1/2} & y \in (y_{T,k}, y_y], \\ \frac{(y - y_w)}{(y_w - y_y)^2} \left[ u_1^*(3y - 2y_y - y_w) - 6q_1 \frac{(y - y_y)}{(y_w - y_y)} \right] & y \in (y_y, y_w], \end{cases} \quad (101)$$

where  $u_0 = u_0(y, y_w(x))$  is again given by (29). The parameters  $u_1^*$  and  $q_1$  are determined according to continuity and to conserve the unit flow rate; they have the identical meaning as previously, but different expressions.

A number of comments are due. First of all, the expression for the yield surface (99) is completely different to ours, in that  $y_{T,k}(x) < y_y(x)$  always. If we consider  $h = O(\delta)$  then the leading order perturbation of the yield surface disappears and we have  $y_{T,k}(x) \sim y_y(x)$ , for finite  $k > 0$ , i.e. the distinguished limit method does not predict any perturbation of the true yield surface from the pseudo-yield surface, let alone a variation in the true yield surface that is in the opposite sense to that in  $y_y(x)$ .

It might be argued that (99) is better suited to the case  $h = O(1)$ . Indeed, in such fully yielded extensional regions the first order velocity perturbation will coincide with (90). It can be seen that for  $h = O(1)$ , we have  $u_{pp,x} \sim O(1)$  and so the true yield surface may vanish for some interval of  $x$  about the point where  $|u_{pp,x}|$  is maximal. However, there appears to be no reason to expect that (99) has any physical meaning<sup>1</sup> for the exact Bingham model.

<sup>1</sup> Obviously there is physical meaning in this expression if we consider a fluid with rheology that is approximated by the appropriate bi-viscous model

If we believe that  $y_{T,k}$  has meaning as a yield surface of some description, we must ask how  $k$  is to be selected, independently of  $\delta$ . This then is the chief problem with the distinguished limit approach. It is sometimes argued that the limit  $k \rightarrow 0$ , should correspond to the exact Bingham model. Here we see that this argument is erroneous. Taking  $k \rightarrow 0$  in (99) will produce  $y_{T,k} = 0$  everywhere, except where  $y_{w,x} = 0$ . As  $k \rightarrow 0$  the yield surfaces will be found to surround plug regions that are progressively narrow, located about each point of symmetry of the wall variation. However, we have seen that for the exact Bingham model, purely from symmetry arguments, that a true plug region will remain about each point of symmetry, extending out to  $y_y(x)$ . From our asymptotic solution, we have argued that these regions should have width  $\sim O(\delta^{1/2})$  when  $h \sim O(1)$ . Thus, selection of  $k$  cannot be independent of  $\delta$  if it is to correctly represent the true plug region.

## 6 Discussion

The main contribution of this paper has been to develop an asymptotic solution for the Poiseuille flow of a Bingham fluid down a channel of slowly varying width, in the case that the variation is small. This helps clarify the limit of small amplitude  $h$ , where intuitively one would expect that the plug region of the plane channel flow should be recovered.

We have shown that an asymptotic solution with an intact true plug region can be found for  $h$  less than a critical value  $h_c \sim O(\delta)$ , and provided upper and lower estimates for  $h_c$ . The function  $h_c/\delta$  shows little variation with  $\delta \ll 1$ , and exhibits a maximum in  $B$  at around  $B \approx 5$ . In general, there is a small variation in the true plug speed from that of the uniform channel. At small  $B$  the perturbed plug moves slightly slower than that in the uniform channel, whereas at large  $B$  the true plug moves faster than that in the uniform channel.

After the plug breaks the flow consists of three regions: a shear flow layer close to the wall, true unyielded plugs of width  $\sim O(\delta^{1/2})$ , about each point of symmetry of the periodic wall variation, and extensional flow regions in between. In the extensional flow regions the method of [19] is easily adapted to yield the leading order solution.

Although the picture is largely complete, in so far as small amplitude variations are concerned, there are a number of interesting questions in this area remaining to be studied.

- (1) Generalisation of our analysis to channels with non-symmetrical width variations, i.e. determination of the plug speed and a more general plug breaking criteria.

- (2) Confirmation of our analysis by numerical solution. This is difficult for all the usual reasons that computation of problems with high aspect ratio are difficult. However in addition, an algorithm must be used that computes unyielded regions, e.g. the augmented Lagrangian method. Use of an algorithm involving regularisation is likely to lead to numerical results that correspond essentially to the bi-viscous model solution. We have seen that interpretation of yield surfaces in such models is not straightforward.
- (3) Asymptotic analysis of the case,  $h \sim h_c$ , just after the plug has broken. Since the plug breaks at  $x_p$ , the two broken pieces will no longer be constrained to move at speed  $u_{pp}(x)$ . Presumably there is some form of relaxation. Determination of the new plug speeds and study of transition to the case  $h \sim O(1)$  would be of interest.
- (4) Identification of the shape of the true yield surfaces for the case  $h \sim O(1)$ , shown schematically in Fig. 14.
- (5) Consideration of large  $h$ , wherein fluid may become stuck on the wall in the wide parts of the channel. This is likely to be associated with flow reversal.

**Acknowledgements:** This research has been supported financially by Schlumberger and NSERC through CRD project 245434, as well as by the Pacific Institute for the Mathematical Sciences. This support is gratefully acknowledged. S.K. Wilson and B.R. Duffy are thanked for their hospitality and for helpful friendly discussions of the method in §5, and consideration of the extensional flow after breaking of the plug, all during a study visit to the University of Strathclyde in August 2002, (IF). R. Craster is thanked for his lucid explanations of [19].

## References

- [1] G.G. Lipscomb and M.M. Denn Flow of Bingham fluids in complex geometries. *J. Non-Newtonian Fluid Mech.*, 14 (1984) 337-346.
- [2] I.C. Walton and S.H. Bittleston, The Axial Flow of a Bingham Plastic in a Narrow Eccentric Annulus. *J. Fluid Mech.* 222 (1991) 39-60.
- [3] P. Szabo and O. Hassager, Flow of Viscoplastic Fluids in Eccentric Annular Geometries. *J. Non-Newtonian Fluid Mech.* 45 (1992) 149-169.
- [4] G.H. Covey, and B.R. Stanmore, Use of the parallel-plate plastometer for the characterisation of viscous fluids with a yield stress. *J. Non-Newtonian Fluid Mech.*, 8 (1981) 249-260.
- [5] E.J. ODonovan and R.I. Tanner, Numerical study of the Bingham squeeze film problem. *J. Non-Newtonian Fluid Mech.*, 15 (1984) 7583.

- [6] D.K. Gartling and N. Phan-Thien, A numerical simulation of a plastic fluid in a parallel-plate plastometer. *J. Non-Newtonian Fluid Mech.*, 14 (1984) 347360.
- [7] S.D.R. Wilson, Squeezing flow of a Bingham material. *J. Non-Newtonian Fluid Mech.*, 47 (1993) 211219.
- [8] J.D. Sherwood and D. Durban, Squeeze flow of a power-law viscoplastic solid. *J. Non-Newtonian Fluid Mech.*, 62 (1996) 35-54.
- [9] J.D. Sherwood and D. Durban, Squeeze-flow of a HerschelBulkley fluid. *J. Non-Newtonian Fluid Mech.*, 77 (1998) 115-121.
- [10] D.N. Smyrniaios and J. Tsamopoulos, Squeeze-flow of Bingham plastics. *J. Non-Newtonian Fluid Mech.*, 100 (2001) 165-190.
- [11] K.F. Liu and C.C. Mei, Slow Spreading of a Sheet of Bingham Fluid on an Inclined Plane. *J. Fluid Mech.* 207 (1989) 505-529.
- [12] K.F. Liu and C.C. Mei, Approximate equations for the slow spreading of a thin sheet of Bingham plastic fluid. *Phys. Fluids*, A2 (1990) 30-36.
- [13] P. Coussot and S. Proust, Slow, unconfined spreading of a mud flow. *J. Geophys. Res.*, 101 (1996) 25217-25229.
- [14] P. Coussot, S. Proust and C. Ancey, Rheological interpretation of deposits of yield stress fluids. *J. Non-Newtonian Fluid Mech.*, 66 (1996) 55-70.
- [15] J.M. Piau, Flow of a yield stress fluid in a long domain. Application to flow on an inclined plane. *J. Rheology*, 40 (1996) 711-723.
- [16] R.W. Griffiths and J.H. Fink, Solidifying Bingham extrusions: A model for the growth of silicic lava domes. *J. Fluid Mech.*, 347 (1997) 13-36.
- [17] X. Huang and M.H. Garcia, A Herschel-Bulkley model for mud flow down a slope. *J. Fluid Mech.*, 374, (1998) 305-333.
- [18] S.D.R. Wilson and S.L. Burgess, The steady, spreading flow of a rivulet of mud. *J. Non-Newtonian Fluid Mech.*, 79 (1998) 77-85.
- [19] N.J. Balmforth and R.V. Craster A consistent thin-layer theory for Bingham plastics. *J. Non-Newtonian Fluid Mech.*, 84 (1999) 65-81.
- [20] S.D.R. Wilson, A note on thin-layer theory for Bingham plastics. *J. Non-Newtonian Fluid Mech.*, 85 (1999) 29-33.
- [21] R.W. Griffiths The dynamics of lava flows. *Annu. Rev. Fluid Mech.*, 32 (2000) 477-518.
- [22] N.J. Balmforth, A.S. Burbidge, R.V. Craster, J. Salzig, & A. Shen, Visco-plastic models of isothermal lava domes. *J. Fluid Mech.*, 403 (2000) 37-65.
- [23] N.J. Balmforth and R.V. Craster Dynamics of cooling domes of visco-plastic fluid. *J. Fluid Mech.*, 422 (2000) 225-248.

- [24] C.C. Mei and M. Yuhi, Slow flow of a Bingham fluid in a shallow channel of finite width. *J. Fluid Mech.* 431 (2001) 135-159.
- [25] A.B. Ross, S.K. Wilson, and B.R. Duffy, Thin-film flow of a viscoplastic material round a large horizontal stationary or rotating cylinder. *J. Fluid Mech.* 430 (2001) 309-333.
- [26] S.K. Wilson, B.R. Duffy and A.B. Ross, On the gravity-driven draining of a rivulet of viscoplastic material down a slowly varying substrate. *Phys. Fluids* 14 (2002) 555-571.
- [27] S.D.R. Wilson and A.J. Taylor, The channel entry problem for a yield stress fluid. *J. Non-Newtonian Fluid Mech.*, 65 (1999) 165-176.
- [28] M.A.M. Al Khatib and S.D.R. Wilson, The development of Poiseuille flow of a yield stress fluid. *J. Non-Newtonian Fluid Mech.*, 100 (2001) 1-8.